BATTERIES AND THERMAL ENERGY STORAGE:

AN ANALYTICAL METHOD FOR SIZING AND

ANALYZING POTENTIAL SYNERGIES

IN HYBRID SYSTEMS

by

Matthew Brandt

A thesis submitted to the Faculty and the Board of Trustees of the Colorado School of Mines in partial fulfillment of the requirements for the degree of Master of Science (Mechanical Engineering).

Golden, Colorado

Date _____

Signed: _____

Matthew Brandt

Signed: _____

Dr. Paulo Cesar Tabares-Velasco
Thesis Advisor

Signed: _____

Dr. Jason Woods
Thesis Advisor

Golden, Colorado

Date _____

Signed: _____

Dr. John Berger
Professor and Department Head
Department of Mechanical Engineering

ABSTRACT

Electric-grid generation capacity is sized to meet the peak load, typically in the summer when building cooling loads are high and is underutilized for much of the year. Electric utilities often pass on the costs associated with these peaking generators to building owners through demand charges. Building owners can minimize these demand charges by shifting energy use away from peak periods with behind the meter storage. This storage can include batteries, which can directly shift the metered load, or thermal energy storage, which can shift thermal-driven electric loads like air conditioning. However, there is a lack of research on how best to combine battery and thermal energy storage.

In this study, an analytical sizing method is developed for a hybrid system, calculating the potential demand reduction and annualized cost savings for different combinations of thermal and battery energy storage sizes. It is shown that adding batteries to a thermal energy storage system increases the total system's load shaving potential. This is particularly true when the building has onsite PV generation or electric vehicle charging, which add significant variability to the load shape. It is also shown that for a given total storage size, selecting a higher fraction of thermal energy storage can significantly lower the cycling of the battery, and therefore extend the battery life. This, combined with the expected lower first cost of thermal energy storage materials compared to batteries, shows that hybrid energy storage systems can outperform a standalone battery or standalone thermal storage system.

TABLE OF CONTENTS

LIST OF FIGURES

LIST OF TABLES

LIST OF SYMBOLS

Nomenclature	**Meaning**
ACC_{ES}	Annualized capital cost of energy storage system
ACS	Annual cost savings
CC_{ES}	Total capital cost of energy storage system
COP	Coefficient of performance
$\overline{COP_{\mathrm{discharge}}}$	Discharge-power-weighted average coefficient of performance of TES discharge
$\overline{COP_{\mathrm{charge}}}$	Charge-power-weighted average coefficient of performance of TES charge
$\overline{COP_{\mathrm{base}}}$	Power-weighted average coefficient of performance of baseline equipment during TES discharging timesteps
E	Electrical energy input/output to device/system
E_{avoided}	Metered electrical energy decrease resulting from discharging energy storage system
E_{supplied}	Metered electrical energy increase resulting from charging energy storage system
$E_{\mathrm{discharge}}$	Electrical energy discharged from storage system
E_{charge}	Electrical energy charged into storage system
E_{base}	Electrical energy required to meet total or thermal loads in the absence of an energy storage system
l_{ES}	Lifetime of energy storage system
p_{D}	Price of demand charge
p_{E}	Price of energy for a flat rate structure
p_{L}	Price of energy during off-peak (low) period for a time-of-use rate structure

p_{H} ..... Price of energy during on-peak (high) period for a time-of-use rate structure

PS_m ..... Maximum possible peak demand shaving that can be achieved in month m

Q ..... Thermal energy input/output to device/system

$Q_{\mathrm{discharge}}$ ..... Thermal energy discharged from storage system

Q_{charge} ..... Thermal energy charged into storage system

r ..... Discount rate

t_{shave} ..... Total time (sum of all timesteps) for which storage is discharging

$t_{\mathrm{shave,max}}$ ..... Maximum time of peak demand shaving for which storage results in utility cost savings

UCS ..... Utility cost savings

Δd ..... Incremental decrease in demand power resulting from storage discharge

β ..... Fraction of total discharge energy delivered by battery energy storage

τ ..... Fraction of total discharge energy delivered by thermal energy storage

η_{ES} ..... Electrical round-trip efficiency of an energy storage system

η_{BES} ..... Electrical round-trip efficiency of a battery energy storage system

η_{TES} ..... Electrical round-trip efficiency of a thermal energy storage system

η_{HES} ..... Electrical round-trip efficiency of a hybrid energy storage system

$\eta_{\mathrm{TES,th}}$ ..... Thermal round-trip efficiency of a thermal energy storage system

Abbreviations	Meaning
APUP	Alliance partner university program
ASHP	Air-source heat pump
BES(S)	Battery energy storage (system)
BTM(S)	Behind-the-meter (storage)
CHP	Combined heat and power
COP	Coefficient of performance
DCFC	Direct current fast charging
DER-CAM	Distributed energy resources customer adoption model
EFC	Equivalent full cycles
EV	Electric vehicle
EVI-Pro	Electric vehicle infrastructure projection tool
EWH	Electric water heater
GSHP	Ground-source heat pump
HES(S)	Hybrid energy storage (system)
HP	Heat pump
HPWH	Heat pump water heater
HVAC	Heating, ventilation, and air conditioning
LDC	Load duration curve
LP	Linear programming
MILP	Mixed-integer linear programming
MINLP	Mixed-integer nonlinear programming
MPC	Model predictive control

NREL .....National Renewable Energy Laboratory

PCM .....Phase change material

PV ..... Photovoltaic

REopt .....Renewable Energy Integration and Optimization

SAHP .....Solar-assisted heat pump

SAM.....System advisor model

SOC.....State of charge

TES(S).....Thermal energy storage (system)

TMY..... Typical meteorological year

TOU .....Time-of-use

USD.....United States dollar

CHAPTER 1

INTRODUCTION

Buildings account for 75% of U.S. electricity consumption and 40% of total U.S. energy consumption [1]. Space conditioning, particularly building cooling during summer months, is a dominant factor in this consumption, accounting for about 32% and 53% of the total energy consumed by commercial and residential buildings, respectively [2]. The impact of buildings on the electric grid is only going to increase as renewable energy and building-supported electric vehicle (EV) charging stations become more common. Renewable energy generation is continuously increasing on both the supply and demand side. However, wind and solar are inherently variable, which increases electric grid challenges to reliably meet the demand. In addition, electric vehicle (EV) use is increasing, which may increase the electric demand power for buildings if the meter is shared. For example, California plans to have 250,000 EV charging stations by 2025 [3], and Colorado has a goal to have almost 1 million EVs by 2030 [4].

The increased load from EV chargers, along with increased renewable energy capacity, will drive the need for flexible resources to balance supply and demand on the electric grid. Energy storage is expected to play an important role in this task by improving building flexibility and altering electric energy consumption patterns based on needs from utilities. Utilities can encourage the use of energy storage by imposing variable rate structures that promote consuming more energy during off-peak periods and less during on-peak periods. Two common variable rate structures are (1) time-of-use energy rates, in which the energy price during peaking periods is greater than the off-peak energy price and (2) demand charges, which are assessed on the peak demand power in either an on-peak period or for all time throughout the billing cycle (or both).

Behind-the-meter (BTM) energy storage, in which energy storage assets are owned and controlled by the customer, typically consists of electrochemical batteries and thermal energy storage. Battery energy storage (BES) costs are declining, but still tend to be more expensive than a comparable thermal energy storage (TES) system due to higher capital expense, faster life-cycle degradation, and potentially higher operation costs [5]–[8]. Batteries are considered more flexible since they directly meet the electrical load for which the consumer is billed [9]. In contrast, TES uses less expensive materials than batteries (e.g., water/ice tanks) and therefore typically has a lower first cost [10] but can only be used to address thermal loads and not nonthermal loads like EV charging or building electric loads like plug loads and lighting. Since cooling drives peak demand on the grid and typically coincides with the periods of on-peak electricity rates, cold TES can still make significant contributions to peak management. These differences between batteries and TES make any direct comparison or operating decision challenging—there are no standard methods to guide the process of selecting, sizing, or controlling these two assets together to maximize energy cost savings. While many studies have developed approaches for optimizing a single storage type, relatively few have considered the tradeoffs and benefits from using a hybrid battery/TES system.

The limited research that does exist shows strong potential for hybrid energy storage systems compared to a single-type storage system. One key limitation is that most studies implement optimization approaches. Optimization results can be difficult to generalize, and the influence of different factors must be analyzed on a case-by-case basis. Furthermore, the sophisticated software utilized for advanced energy optimizations may not be publicly available, and so studies involving optimizations are typically in-house studies at large research facilities (e.g., REopt at National Renewable Energy Laboratory). Finally, the majority of these software

tools utilize mixed-integer linear programming (MILP), so physical phenomena must be linearized, which could impact the fidelity of results. By comparison, analytical techniques can obtain similar solutions with lower programming and computational overhead. Analytical techniques can complement optimizations by addressing some of the potential drawbacks described above, especially in (1) directly relating inputs and outputs in concise formulations and (2) capturing nonlinear phenomena by integrating high-fidelity physics-based models that do not need to be linearized. For example, Wu et al. from Pacific Northwest National Laboratory (PNNL) demonstrate an analytical approach to sizing batteries and obtain a solution within 1% of the optimization-based result [11]. Wu et al.'s procedural approach compares the incremental utility cost savings with the incremental capital costs for larger and larger batteries to find the maximum useful battery size. Thus, the authors directly relate the pseudo-optimal power and energy capacities to the load profiles, utility rate structures, and capital costs. An important drawback of their analysis is that they analyze a peak day, rather than analyzing the load profile throughout a month (which is the typical billing cycle). Their study also does not consider the impacts of other BTM assets such as EV charging and PV, but the analysis could be easily repeated to address this gap.

This thesis extends Wu et al.'s analytical approach for application with hybrid systems composed of batteries and thermal energy storage. This new approach is demonstrated for a simulated big-box grocery and retail building with different combinations of other BTM assets such as PV and EV charging stations. The results from this example study suggest potential synergies between batteries and thermal storage exist, by which the building owner can take advantage of differences in capital cost, flexibility, and sensitivity to life-cycle degradation to achieve better outcomes than obtained with a stand-alone system.

In summary, the overall objectives of this research are to:

i. Modify and improve upon Wu et al.'s analytical method to size a hybrid energy storage system based on the utility rate structure, energy storage system characteristics (e.g., efficiencies, capital costs), and the electric load profiles for the total and thermal electric demand power.

ii. Explore the impacts of other behind-the-meter assets such as PV or electric vehicle charging stations on the useful energy and power capacities of hybrid energy storage systems.

iii. Identify potential synergies between batteries and thermal energy storage, which account for possible factors such as

    a. Applicability to different kinds of electric loads

    b. Sensitivity to cycling

    c. Capital costs and storage system lifetime

    d. Utility rate structures

This thesis is divided in the following chapters:

- CHAPTER 2 BACKGROUND AND SIGNFICANCE: This chapter reviews the current literature regarding battery energy storage, thermal energy storage, and hybrid systems. Special focus is given to BTM storage. This chapter is a reproduction of a literature review submitted to National Renewable Energy Laboratory (NREL) as one deliverable for the Alliance Partner University Program (APUP) agreement funding this work.
- CHAPTER 3: MODEL INPUTS: This chapter describes the inputs required for the proposed analytical method and provides details on the building energy, EV charging, and PV modeling used to create total and thermal electric load profiles to demonstrate the analytical method. The

building total and thermal electric demand power profiles were produced in EnergyPlus and the EV charging profile was created in EV EnSite. Both the building and EV models were provided by NREL. The PV generation profile is developed using NREL's System Advisory Model (SAM).

- CHAPTER 4 ANALYTICAL METHODS FOR SIZING AND IDEALIZED DISPATCH: This chapter describes the proposed analytical approach utilized to size and analyze hybrid energy storage systems. Key differences and improvements between other analytical methods in the literature are discussed, including the application of a binary search method which is both flexible and computationally efficient.
- CHAPTER 5 RESULTS: This chapter discusses the application of the new analytical approach to a simulated big-box grocery and retail store, the relevance of the load profile shape in behind-the-meter analysis (using load duration curves), and potential synergies between battery energy storage and thermal energy storage systems.
- CHAPTER 6 CONCLUSIONS: This chapter presents a summary of significant results and suggestions for future research based on this work.

CHAPTER 2

BACKGROUND AND SIGNIFICANCE

Given the increasing need for energy storage resulting from changing building needs, EV charging stations, and variable renewable energy generation, there has been a significant amount of research effort focused on batteries and thermal energy storage systems in recent years. Many studies develop optimization approaches for a single kind of storage system [12]–[15]. Others consider tradeoffs between using one kind of energy storage or another, such as comparing batteries against thermal energy storage [16]–[20]. However, there are relatively few studies considering synergies of hybrid energy storage systems by simultaneously using a combination of electrochemical and thermal energy storage systems. Further study of hybrid systems is critical because benefits exceeding stand-alone systems may be possible when a user combines dissimilar storage systems and develops controls based on each system's unique power and energy characteristics and varying capital and operational costs [21]–[24].

Energy storage is an extremely diverse topic with a wide range of applications and objectives. Grid-side goals can include increasing flexibility, improving resiliency, or load levelling. Load duration curves, in which load profiles are sorted in a descending order over a billing cycle or other period of interest, are regularly used as part of defining metrics concerning energy generation resources and to predict the potential benefits of grid-scale storage for grid-side goals such as load flexibility and load levelling. Meanwhile, BTM studies typically emphasize customer cost savings under a given electricity rate structure, accomplished by using the storage for load levelling, energy shifting, or peak demand shaving; however, the applicability of load duration curves to hybrid systems from a demand-side perspective remains to be seen.

This literature review focuses on behind-the-meter storage (BTMS) for demand reduction and/or energy shifting to support NREL's BTMS project. One of the goals of this project is characterizing the impacts on storage utilization potential associated with adding electric vehicle charging stations and/or renewable resources as a function of the electricity rate structure (and other variables such as building type and climate). This chapter provides a brief overview of current studies on energy storage for demand reduction and energy shifting. This includes a quick overview of studies on electrochemical energy storage, followed by a discussion of thermal energy storage for both cooling and heating applications. Special attention is given to studies on heating applications, particularly those utilizing heat pumps and phase change materials, since this is one TES type proposed to limit future peak demand in winter when the US economy is decarbonized. The review concludes by documenting hybrid systems that combine batteries with thermal energy storage systems for both cooling and heating applications.

2.1. Electrochemical (battery) energy storage

Batteries can be used for different applications and have seen significant improvements in energy and power capacity resulting from substantial research in the last several decades. Batteries typically have several advantages over TES. They are able to directly meet the electrical load at the meter for which the consumer is billed; in contrast, TES systems operate on a thermal load, for which the consumer is not directly billed. Consequently, they are generally considered more flexible and have greater load-levelling potential [9]. However, batteries tend to be more expensive than a comparable thermal storage system due to higher capital expense, faster life-cycle degradation, and potentially higher operation costs [5]–[8]. Being an energy storage asset, coordination between charging and discharging is key to improve savings and battery lifetime. Battery control and sizing have been the subject of substantial research effort, both in terms of

grid- and customer-side load management using both optimization and rule-based approaches as summarized in numerous review papers (e.g., [25]–[28]). A few studies are presented below which highlight some limitations of batteries.

Neubauer et al. find that small, short-duration batteries are the most likely to be cost effective for typical commercial facilities based on current electricity pricing and incentives [29]. In their analysis, the battery shaves only around 2.5% of the peak power demand at the meter. Wu et al. use a linear programming approach to optimally size a BTM battery storage system and conclude that the optimal size of power and energy capacities primarily depends on the load profile, electricity rate tariffs, and battery cost [30]. Based on the optimization results, Wu et al. develop a simplified "analytical" approach for sizing, which depends on the factors that were found to be the most important from their earlier work [31]. The analytical method yields the same optimal energy capacity and C-rate as the linear programming method when annualized capital cost (as a function of both energy and power) is used to constrain the battery sizing. This is a key finding, as analytical solutions are simpler to code and could provide an optimal or near-optimal solution without the cost of implementing complex optimization formulations. Furthermore, using load duration curves in these behind-the-meter studies may represent one way to more easily visualize contributions of factors in optimal power and energy sizing [32].

Zurfi et al. similarly find that the optimal BTM battery storage system capacity is impacted primarily by the battery cost versus the savings that can be achieved under a given rate structure for a two-story residential building in Arkansas [33]. The paper finds that utilizing BES is not generally profitable for residential peak demand shaving with a demand charge of 12 USD/kW or less. Chen et al. use a day-ahead black-box optimization algorithm to obtain 13% reduction in operation costs for a medium-sized office under TOU utility rates [34]. Many other studies have

found that the most important factors for battery sizing are the interplay between capital cost and electricity rate structure, which are more important than other factors such as PV size or battery performance [35], [36]. For example, Heine et al. conclude that sizing batteries 1.5 to 1.6 times larger than required to meet the annual peak energy purchase requirements provides maximum NPV for PV-battery systems at locations with favorable (and variable) utility rates [37].

These studies underscore the limitation that batteries currently have a high capital cost but offer greater flexibility in directly meeting demand for which the customer is billed. Therefore, hybrid systems composed of batteries and TES must be analyzed, since they may benefit from the compromise between the flexibility of batteries and the cost-effectiveness of TES. More importantly, the study by Wu et al. shows that an analytical solution that can optimize battery size is plausible. The study did not consider any hybrid systems [31].

2.2. Thermal energy storage

A significant amount of research has also been performed in terms of materials, systems integration, and performance for thermal energy storage for both cooling and heating applications, as summarized in recent literature reviews (e.g., [38]–[42]). Compared with batteries, thermal storage systems generally have a lower capital cost [10]; however, TES systems have a number of drawbacks. The energy stored is of a lower exergetic quality than electrical energy, and a TES system has greater stand-by losses than batteries [43]. The most common materials for storing cool thermal energy are ice/chilled water or precooled building thermal mass. Building heating studies have primarily involved hot water storage, sensible storage in building thermal mass (e.g., brick and concrete), or solid-liquid PCMs. However, this review focuses on behind-the-meter energy shifting with special attention to studies involving heat pumps and PCMs.

For BTM TES systems focused on electricity load management, Arteconi et al. compile a summary of key benefits (see Table 2.1) offered by TES systems for both heating and cooling applications and categorized their benefits in terms of systems and operating benefits. Table 2.1 shows that typical building HVAC components can be downsized by up to 40% with the addition of a TES medium. This downsizing also typically results in higher device efficiencies. The customer benefits by receiving lower equipment and electricity costs but without any impact on thermal comfort.

Table 2.1 TES demand-side management benefits, modified from Arteconi et al. [44]

Category	**Benefit**
HVAC systems	
Cooling	Smaller size of unit (up to 40%)
	Improved efficiency
	Smaller air handling units (up to 40%)
	Reduction of building structural cost (up to 3%)
	Reduction of thermal loads
Heating	Increased performance
	Size reduction
Building owner and occupants	Lower equipment costs
	Lower electricity costs
	No change in thermal comfort

Building TES applications are typically focused on cooling since it currently drives the electric peak consumption during summer. Concerns related to human-driven climate change and the resulting increased use of air conditioning further underlines the need for research on managing electric demand power under continually increasing cooling requirements. Arteconi, Sun, Aziz, Guelpa, and Faraj et al. provide thorough reviews of TES for cooling applications [38], [40], [44]–[46].

Precooled building mass and PCMs are also used as storage media. Precooling generally increases energy consumption, but the time-shift can result in savings if the electricity rate structures include TOU rates and/or demand charges [21]. Several studies found that the length of the on-peak period affects the total energy shifted (as expected), where 5-hours allowed peak demand reduction of up to 30%. Narrowing the on-peak period to 3-hours led to demand reduction of up to 80% [47]–[52]. Sun et al. provide a summary of simulation and experimental studies on precooling, summarized in their Table 1 [21]. Faraj et al. provide a comprehensive review of PCM TES systems for cooling applications [38].

The literature on cooling storage is broader than for heating applications; however, recent trends are likely to lead to renewed interest in heating. As the economy, states, and local governments seek to limit their carbon footprint, there is a major trend toward building electrification by replacing gas heating equipment with electrical heating options such as heat pumps. Building electrification in this space may have significant consequences for the grid, considering buildings are already responsible for 75% of U.S. electricity consumption. Adding to the challenge, buildings' electricity share will only increase as building-supported electric vehicle charging stations adoption expands [53], [54]. Using a TES system is expected to play an important role in mitigating the effects of building electrification, particularly from the utilization of heat pumps, electric water heaters, and other means to limit the natural gas consumption of buildings associated with water and space heating. See [39], [42], [55], [56] for an overview of current studies on heating applications.

Table 2.2 presents an overview of studies involving heat pumps paired with a sensible or latent thermal storage. Table 2.2 demonstrates that, although both air-source and ground-source heat pumps have been studied extensively, their application with TES is generally limited to water

Table 2.2 Overview of Heat Pump + TES studies (see LIST OF SYMBOLS for abbreviations used in this table)

Ref	HP Type	Storage Description	Study Objective	Rate Structure	Software / Methods	Results / Conclusions / Other
[62]	ASHP	Generic (Lumped Capacitance)	Load flattening, grid stability	N/A	MILP	Adding EHP and TES reduced maximum power difference from 40.9 kW to 32.7 kW, about 20%.
[63]	ASHP	PCM in finned tube	Energy shifting from on-peak period	TOU	Experimental	With improved heat transfer, storage size (for full shifting) reduced by 30%.
[64]	ASHP	PCM in concrete floor slab	System COP and internal T variations in multiple climates; compare energy/CO_2 against flat rate, TOU, and gas boiler	TOU	TRNSYS	All combs of system had lower operating costs and CO_2 emissions compared to gas boiler, annualized COP reached 4 (mild climate) and 3.5 (cold climate) for E10, and E7 increased electricity requirement by 11-15%.
[59]	ASHP	PCM + Water tank	Impact of PCM on storage volume	TOU	ESP-r	PCM reduces required volume by factor of 2 for full shifting.
[60]	ASHP	PCM + Water tank	Impact of PCM on storage capacity	N/A	Experimental	Storage capacity increased by 14% with minimal change to tank volume.
[65]	ASHP	Thermal mass	Maintain room setpoint temp	TOU	Matlab / Simulink	Validated modeling.
[58]	ASHP	Thermal mass and Stratified Hot Water Tank	Flexibility with different configs of HP and TES	RT/TOU	TRNSYS	Load shifting potential indicator developed which suggests TES most useful for bulk energy shifting. Energy efficiency devices most useful for strategic conservation and peak shaving.
[66]	ASHP	Stratified Hot Water Tank	Minimize electricity costs by energy shifting from on-peak period	TOU	TRNSYS	Under TOU rates (~3x ratio), HP+PCM can economically shift load. With HP and buffer (no PCM TES), full shifting achieved in on-peak. With HP and PCM, 85% load shifted out of on-peak.
[67]	ASHP	Water tank	Energy shifting from on-peak period caused by transition from gas boilers to heat pumps	TOU	Multi-objective MPC	Model of 500,000 buildings in Belgium with heat pumps allows 11% reduction of peak load power supply by grid, but operational costs increase to consumer

Table 2.2 Continued

[68]	ASHP	Water tank	Modified evaporator to solve the mass non-conservation problem existing in common evaporator models	N/A	Numerical	Water heating rate and consumption increased by 40% and 10% respectively when compressor frequency increased from 40 to 60 Hz. Validated modeling
[69]	ASHP + Gas Boiler	Water tank	DR indicators for flexibility, control algorithm for HESS	TOU	NLP used for MPC	TES with TOU resulted in reduced load-share covered by boiler from 33% to 0.3%; TES+TOU led to 8% cost saving and 13% reduction of energy
[70]	GSHP	--	Model of GSHP in context of whole building energy simulation	N/A	IDA-ICE	Validated modeling.
[71]	GSHP	Water tank	Optimal system selection to minimize life-cycle costs	N/A	PS Optimization	For operating period of 20 years, optimized sizing reduces investment cost by 10% while COPs were reduced by 13% (heat pump) and 11% (system).
[61]	GSHP	PCM + Water tank	Energy shifting from on-peak period	TOU	FORTRAN	50% and 75% PCM reduces req volume by factor of 2.5 and 3, respectively, for full shifting.
[72]	GSHP	PCM + Water tank	Impact of PCM on storage volume	N/A	TRNSYS	TES can completely offset peak demand for 2-6 hours; max error between numerical/analytical was 13%; hybrid PCM reduces req volume by 1/3; TES "not an energy efficiency solution" but reduces CO_2
[58]	GSHP	Stratified water tank + underfloor heating	Flexibility with different configs of HP and TES	RT/TOU	TRNSYS	Load shifting potential indicator developed which suggests TES most useful for bulk energy shifting, energy efficiency devices most useful for strategic conservation and peak shaving.
[73]	SAHP	Water tank	Quantify system characteristics	N/A	--	Collector efficiency: 33-47%, HP COP 3.8 and COP system 2.9
[74]	SAHP	Water tank	Quantify system characteristics	N/A	--	Collector efficiency: 70%, HP COP 4.5 and COP system 4.0
[75]	SAHP	Underground water tank + soil	Determine effects of water stratification wrt tank+temperature field	N/A	Experimental / Numerical	Only top of tank should be insulated since heat contribution from soil can be up to 15%. Validated modeling.

tanks or storage in building components via radiant heating. This review found only one study considering the effects of latent energy storage in the condensing section of the heat pump [57], that TES is generally most useful for bulk energy shifting [58], and that PCMs can reduce the storage volume needed to shift energy by a factor of 2-3 [59]–[61].

2.3. Hybrid systems

Hybrid energy storage systems combine multiple energy storage systems with the objective of obtaining larger benefits with the hybrid system than the individual components achieve. Such synergy may be obtained by utilizing differences in capital or operating expenses, flexibility constraints, or dissimilar power and energy performance characteristics. However, combining systems also requires system coordination to maximize benefits, representing a challenging controls problem in existing systems. Although there are not as many studies analyzing hybrid systems, the ones that have been published tend to focus on formal optimization in sizing and controlling each component in the hybrid system. Various optimization approaches have been used, including linear programming (LP) [76], mixed-integer linear programming (MILP) [77]–[82], mixed-integer nonlinear programming (MINLP) [83], and metaheuristic approaches such as genetic algorithms and particle swarm techniques [84]–[86].

Ikeda and Ooka compare the accuracy and speed of various algorithms [87]. Metaheuristic methods including differential evolution, self-adaptive learning bat algorithm, and a modified particle swarm method are compared with a dynamic programming method. The modified particle swarm optimization comes within 1% of the theoretical optimum control and is 62,000 times faster than the dynamic programming method. Thus, although most studies involving hybrid systems have considered sizing and controls from a formal optimization perspective (especially MILP), new insights may be gained from further study of rule-based and metaheuristic methods which are

less computationally intensive. See Gelleschus et al. for additional discussion of different optimization solvers [88].

There are also publicly available and research-oriented software platforms that have the capability of analyzing some of these systems. They allow users to optimize any combination of an arbitrary set of storage devices, whether they are dissimilar batteries, combinations of multiple TES systems, or a combination of electrochemical and thermal energy storage. These programs are most frequently developed using an MILP approach, such as in NREL's REopt and Foresee and LBNL's DER-CAM, but there are other "energy hub" platforms [89]–[95], which may not be as user-friendly or may not be available online. Among them, Ashouri et al. develop a "Smart Building Designer" that uses MILP for optimizing various BTMS assets, including BES, TES, and other storage systems (e.g., compressed air) [96]. A case study presents results using the framework for a commercial building in Zurich, which demonstrates the dependence of optimal device selection on the device costs, electricity tariffs, and governmental legislation.

2.3.1. Hybrid systems for cooling applications

Several studies have compared the effects of combining an active cool TES with cool energy storage in the building thermal mass, which is accomplished by precooling strategies and setpoint control. Henze et al. find that using an active TES system (dedicated chiller and ice tank) and precooled building thermal mass under a rate structure with a TOU ratio, the ratio of the high energy price to the low energy price, of 4 (with no demand charges) and optimized with a dynamic programming approach, the hybrid system results in electricity cost savings up to 46% [22]. What is more, this study found the hybrid storage system achieved higher savings than any of the individual systems but was lower than arithmetically adding the savings from each individual technology. Unfortunately, other studies find lower total electricity cost savings. Kintner-Meyer

suggest potential savings of 18% [97]. Hajiah and Krarti find savings of only 10%, even though (as compared to Henze et al.) the TOU ratio is higher and demand charges are present in the electricity rate structure [23], [24]. Although both Hajiah et al. and Henze et al. consider commercial buildings with ice and building mass storage, the studies differ in that Henze et al.' s building is about five times larger. The climate zones also differ; whereas Henze et al. consider a structure in Phoenix, AZ, the Hajiah study is based on data from Boulder, CO which has a shorter cooling season. Yan et al. study the effects of combining ice storage and chilled water storage for a building in Beijing, which decreased annual electricity consumption by 20% and operational costs by 76% [98]. Song et al. also considered ice and chilled water from the perspective of space savings, noting that ice has a higher storage density due to the phase change. They find that adding ice storage to a system with chilled water can have a simple payback of less than 10 years under certain use cases and suggest that the hybrid system can improve economy for high-density building complexes [99]. In all cases, these studies show greater cost savings when utilizing a hybrid system than when using only one component of the storage system.

Relatively few studies specifically optimize combinations of batteries and cool thermal energy storage systems. Ice or chilled water are common cold storage media for TES-only applications. In terms of hybrid studies, Wang et al. numerically combine a battery with cold storage (cold water tank), which leads to downsizing both units and improved overall efficiency [100]. A TRNSYS model of a simple off-grid home is used, and the results indicate an overall efficiency gain of 6-10%, depending on assumptions about the cooling load profile. Utilizing a hybrid system, the required battery capacity is reduced by 75%. Hu et al. analyze a stand-alone air conditioner [6]. Hu et al.'s case study for an office building developed in TRNSYS is used to demonstrate that storing cool thermal energy in a chilled water tank leads to a reduction in the

required battery capacity by around 85%. Results indicating that optimally sizing hybrid systems leads to small(er) batteries is consistent with the previous findings that (1) BES-only studies predict that smaller batteries are typically more economical, and that (2) studies comparing storage systems find that TES has lower capital cost than BES. One such study suggested that TES cost is as much as 100 times lower than BES [10]. Hu et al. pair a battery with ice storage for a district cooling system in Singapore with a combination of MINLP and MPC to size and control the hybrid system [101]. In addition to lowering energy costs, the hybrid energy storage system is intended to assist with frequency regulation and operate as a contingency reserve for the grid. The authors identify the opposing time scales and energy capacities of TES and BES as the key to creating a synergistic hybrid system, reducing electric costs by 38% with perfect load and weather forecasting.

Additional studies use precooled building thermal mass as the cold storage medium. Niu et al. use an ARX model to forecast cooling demand combined with an MILP model to minimize operating costs of using batteries with building thermal mass under a TOU rate structure with a ratio of about 3.3 [78]. Operational costs were decreased by 5.3% when only a battery was used; however, utilizing building thermal mass and precooling reduced operational costs by an additional 4.1%, for a total combined savings of 9.4%. Meinrenken and Mehmani find that combinations of battery and TES (building mass) reduce peak demand for a multi-zone office building in New York by 26% and electricity costs by about 11% [102]. The battery-only or TES-only cases did not attain the same amount of peak shaving: TES-only yielded just 2.2% savings in annual electric costs, with a reduction in summer peak demand of under 7%.

Several studies have considered systems which have the ability to provide both/either hot and/or cold thermal energy storage. For example, Kung et al. defined supervisory control stages

for a rule-based control for a battery combined with TES using sensible heat for cooling and heating applications [103]. Results showed higher storage temperatures translate to higher standby losses and decreased total building performance. For example, increasing the tank temperature from 120 °F to 180 °F increased annual total facility energy use by around 10% (see Figure 9 in [103]) even though it increased the theoretical energy storage capacity by around 160%.

Borland et al. show a reduction of grid-buy by over 94% for an experimental residential home in Hawaii [104]. The reduction in grid-supplied electrical energy is accomplished by combining a solar PV array with energy storage comprised of BES and TES and controlling operation of household appliances. The TES includes hot storage (EWH and solar hot water storage) and cold storage via lowering temperature setpoints by more than 16 °F during the day to avoid A/C use in the evenings when PV is not able to supply electricity to the A/C equipment. The combination of energy storage and appliance timing helps increase self-consumption of the PV generation and resulted in 94% reduction in daily grid-buy in and 100% in the winter season.

Vedullapalli et al. optimize the HVAC setpoints and battery control to minimize electricity costs for a small office in Charleston, SC [105]. One aspect of this study is comparing optimization results between MILP and an MPC. As formulated here, the MPC predicts higher cost savings than the MILP. This is because the MPC formulation causes greater discharge during mid- and on-peak periods. Additionally, the MILP unnecessarily discharges storage during the off-peak period. In addition to comparing MILP and MPC, the study compares and contrasts use cases with no BTMS, only a battery, only HVAC control, or a hybrid system. In each case, electricity consumption is subject to a 3-tier TOU rate structure with a maximum ratio of 4.5, while TOU demand charges are also assessed with a maximum ratio of 3. The electricity cost savings with the combined system are higher than the savings with either individual component. Curiously, the savings of the

combined system is also higher than the arithmetic sum of individual components. Unfortunately, the battery energy capacities between use cases are not provided, so an increased energy storage capacity may be the cause of the resulting increase in savings.

2.3.2. Hybrid systems for heating applications

Most studies analyzing hybrid systems for heating applications combine a battery with either an electric water heater tank ([106]–[108]) or heat pump water heater ([84], [109]–[112]). Heat pumps may be more favorable than electric resistance heating due to their higher second-law efficiency, but they tend to have higher capital costs. Only a few studies (e.g., [110], [113]) address optimization or tradeoffs between heat pumps and electric resistance heating. It is also worth noting that the majority of studies involving hybrid systems for heating applications are considering the effects of energy storage on PV self-consumption.

Electric Water Heaters (EWH)

Shukhobodskiy and Colantuono develop a control algorithm for a hybrid system composed of storage heaters (packaged unit of electrical resistance heating and sensible energy storage in a medium such as ceramic or brick), EHW, and a battery in order to minimize CO_2 emissions and peak demand from residential buildings [106]. The algorithm seeks to initiate load-increasing actions (e.g., charging storage) during low CO_2 intensity time periods. The algorithm reduced CO_2 by 30-100% depending on the season.

O'Shaughnessy et al. use REopt to demonstrate that coordinating the dispatch of PV, battery storage, and a "smart" electric hot water heater tank increased system net present value by anywhere from 60-80%, depending on the type of rate structure: TOU electric rates, demand charges, or compensation rates for excess PV sold back to the grid [107]. Interestingly, the optimization algorithm deploys a smart AC unit, PV, battery, and smart water heater when demand

charges (summer demand charge of 13.5 USD/kW and winter demand charge of 9.3 USD/kW) exist, but does not deploy the battery in cases without a demand charge. This suggests that batteries have an important role to play when peak demand charges are present or there is substantial economic motivation, despite their higher costs compared to other technologies. This is also consistent with Zurfi et al.'s finding that current battery costs typically require demand charges above 12 USD/kW to be economically favorable [33].

Gong et al. find that the optimal battery energy capacity is reduced and PV self-consumption is improved in a hybrid system that has a variable power EWH [108]. Their study seeks to minimize extreme load variations associated with PV (e.g., the duck curve). They find that "while traditional systems curtail PV generation," the optimal hybrid system is able to utilize the maximum PV power at all times.

Heat Pump Water Heaters (HPWH)

Baniasadi et al. find the optimal size and coordination of a residential building with a hybrid storage that consists of battery and a water tank connected to a GSHP for sensible heat storage for heating and cooling applications [84]. Optimized sizing uses a particle swarm method, and the optimal control uses MPC. Their validated method shows electricity cost savings over 80% when subject to a TOU tariff structure with a ratio of 3.6 between high and low energy prices. More importantly, the study finds that the hybrid system achieves the highest reduction in electricity cost savings, compared with optimal BES-only or TES-only scenarios. The hybrid system downsized the battery by nearly 30% compared with the optimal BES-only case. However, the TES in the hybrid scenario (i.e., tank volume) was only around 10% smaller than the TES-only optimal size.

Williams et al. numerically analyze multiple homes with PV, battery, and sensible storage using a water tank for space and water heating purposes that is connected to a ground source heat

pump [109]. This parametric study varies the battery capacity and finds that both forms of storage increase the PV self-consumption by 80%. This study also finds that a rule-based control schedule for the GSHP and tank and time of charging leads to a peak reduction of nearly 50% for the 4-person household case study.

Zurmühlen et al. use a genetic algorithm to optimally size batteries and a sensible storage tank for space and water heating [110]. They find that retrofitting a gas boiler with a heat pump is not economically feasible, but for new constructions, configurations with both a battery and EHW are more beneficial than scenarios with only a battery or only a hot water tank. In addition, smaller batteries generally have lower capital and operating costs, and batteries offer greater flexibility since the TES needs to be sized no larger than what is required to meet space and water heating demand.

Steen et al. develop an MILP model for analyzing battery and sensible thermal energy storage hybrid systems. Their software platform, DER-CAM, can model batteries and hot water tanks heated by low temperature sources (e.g., heat pump) or high temperature sources (e.g., CHP), and includes thermal loss calculations based on storage capacity, ambient temperature, and storage temperature [111]. New thermal loss models predict lower thermal losses than the authors' previous study (i.e., previous versions of DER-CAM) [114], and affects DER-CAM decision making at different levels. This includes recommending higher TES implementation in San Diego, but decreased TES use in other cases compared to their previous study. Nevertheless, the authors find that charging and discharging efficiencies play a more important role than thermal losses in optimal sizing.

Wakui et al. also analyze PV, battery, and HPWH [112] using two-stage stochastic MILP for optimally sizing the hybrid system subject to a TOU pricing scheme with a maximum ratio of

3. The study finds that the interaction between excess PV output utilization and the hybrid storage system is also impacted by electric rates but is reduced when considering stochastic analysis compared to deterministic model. Operating costs and export rates are reduced by 4.5-6% and around 15-20%, respectively. For additional studies involving hybrid systems utilizing heat pumps with a focus on PV self-consumption, see [115]–[118].

2.4. Conclusions and recommended areas of research

This chapter reviews the state of the art for behind-the-meter studies analyzing hybrid storage systems and their control approaches, particularly those investigating batteries paired with TES. This review reveals some important learning lessons with respect to BTMS:

Sizing and control

- Optimal sizing of energy storage depends on many factors, but the most important are the load profile, electricity rate structure, and capital costs.
- While load duration curves are commonly used in grid-side analysis, this literature review found only two studies using load duration curves for analysis or visualizing results from a demand-side perspective.
- Multiple studies found that rule-based or metaheuristic approaches for sizing and/or control are plausible. Such approaches yielded results near the theoretical optima, but with significantly less complexity and computational requirements.
- Current studies sizing storage using a rule-based approach have estimated useful storage capacities for either only BES or only TES. No current studies use an analysis of the tariffs and load duration curves to simultaneously size a BES+TES system, despite optimization studies finding that hybrid systems often result in higher savings than can be achieved with a single system.

- Although important progress has been made analyzing hybrid systems, there are still factors and relationships between factors that have not been fully characterized in terms of both sizing and controls.

Flexibility and applications

- Batteries offer greater flexibility than TES since they can directly meet the net electrical load for which the customer is billed.
- Since timescales with BES are generally shorter, BES is useful for grid services such as frequency regulation. TES is generally more suitable for bulk energy shifting purposes.
- Relatively few studies directly link a physics-based TES model with a whole-building energy simulation.

BES and TES hybrid systems

- Hybrid systems are promising since they allow a user to optimize for diverse energy and power characteristics. They may provide greater value (either in cost savings, decreased peak demand, or increased PV self-consumption) than an individual storage system, encouraging more research on synergistic relationships. In some cases, hybrid systems improved efficiency by up to 10% or allowed downsizing the battery (i.e., device with higher capital cost) by up to 85%.
- Hybrid systems also result in added complexity in hardware and software. In particular, it is important to have smart controls that can optimally coordinate these assets depending on what the ultimate goal is (e.g., electricity cost savings, minimize CO_2 emissions, flexibility).
- Analysis of cooling hybrid systems was more common. Analyzed systems have included ice, chilled water, precooling building mass, or PCM. However, there are fewer studies for space heating and BES. Those that do exist primarily focus on increasing PV self-consumption by using hot water storage. Future work should analyze hybrid systems which pair a battery with

the warm thermal storage systems across the range of storage media and system types that have already been studied independently.

- As building electrification with renewables continues to have a greater impact on electric peak demand, BTM energy management is expected to play a more and more important role during winters and evenings. Further research analyzing how energy storage can mitigate these impacts is needed.
- Few studies involving heat pumps for space heating have investigated including PCMs as a packaged system. In particular, this study found only one study in which PCMs were incorporated into the condenser of the heat pump.

Utility rate structures and capital costs

- Studies using a TOU ratio of 3-5 obtain annual electricity cost savings around 10-20%, even after accounting for system capital costs in some cases. This implies that energy storage will likely not produce sufficient savings if the TOU ratio is less than 3.
- Studies using demand charges show that for energy storage to be beneficial, the price must be at least 12 USD/kW (often even higher). One study found that the presence of a demand charge made the difference between whether the optimization algorithm deployed a battery or not.
- Since TES systems generally have a lower capital cost, the optimal peak shaving may be higher with a TES. By comparison, a BES may have optimal peak shaving as low as 2.5%, where small batteries are used to offset brief spikes in the net load.

With these gaps and lessons in mind, this thesis aims to address the lack of an analytical method for sizing and dispatching hybrid energy systems. Based on findings from this review, TES is prioritized for bulk energy shifting, while BES is utilized for meeting nonthermal loads. The example cases presented here focus on peak demand shaving, though the approach is equally

applicable for TOU energy rates. The annual analysis also demonstrates a basic approach for accounting for the impact of capital costs on the potential total cost savings.

CHAPTER 3

OVERVIEW OF ANALYTICAL APPROACH AND DESCRIPTION OF MODEL INPUTS

This chapter introduces the new analytical method for sizing hybrid energy storage systems, and the methodology used to demonstrate this approach with a simulated big-box grocery and retail store with combinations of EV charging stations and PV. Figure 3.1 shows a flow chart of the overall approach, which is also a visual outline of this thesis' methodology and results. The approach requires three primary inputs: (Section 3.1) the variable utility rate structure, (Section 3.2) the energy storage system(s) to be analyzed, including efficiency and performance characteristics, and (Section 3.3) electric demand power profiles at the meter for both the total and thermal loads. In this study, the method is demonstrated using simulated data, so Section 3.3. describes the models used to create the electric load profiles for the big-box grocery and retail building, EV charging stations, and PV generation.

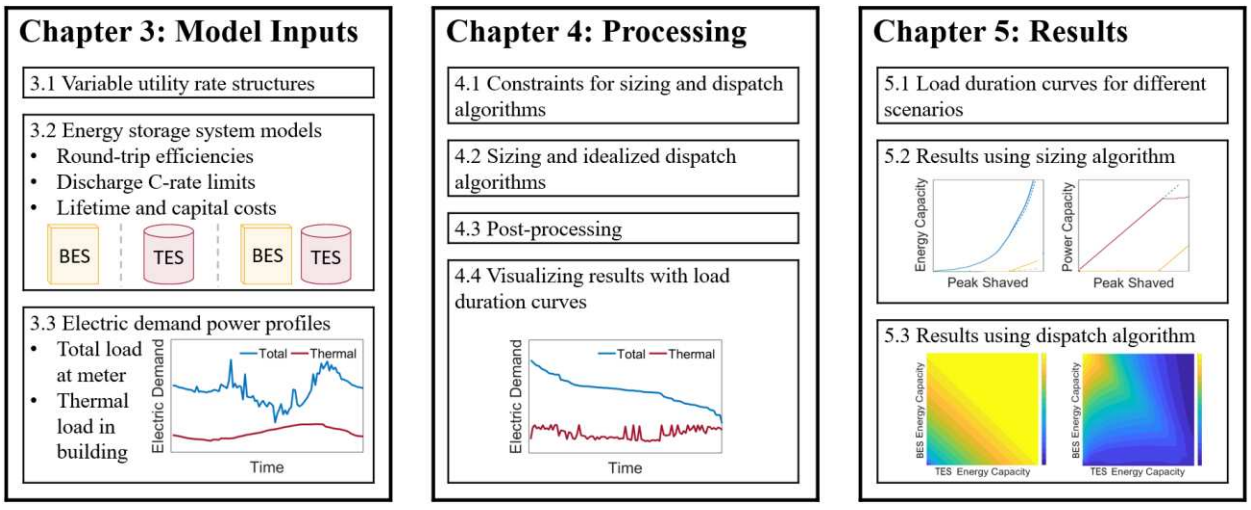

Figure 3.1: A high-level flow chart and visual outline for this thesis which shows the Inputs, Processing, and Results used to explain and demonstrate the proposed analytical sizing and dispatch approach for energy storage systems

Chapter 4 presents a detailed description of the sizing and idealized dispatch algorithms. Both algorithms are subject to constraints derived from the utility rate structure, as described in Section 4.1. The two algorithms are:

1. Sizing algorithm: the minimum energy and power capacities for each energy storage component required to achieve a target monthly peak reduction for a design month.
2. Idealized dispatch algorithm: the maximum possible peak reduction and/or energy shifting for a range of battery and thermal energy storage sizes for a complete year.

See Section 4.2 for a complete description of these two algorithms. Results from the algorithms are post-processed to analyze other outcomes, such as annual utility cost savings, battery cycling, or total cost savings (Section 4.3). Finally, the application of load duration curves for visualizing load shifting results is discussed in Section 4.4.

3.1. Variable utility rate structures

Variable electric rates are needed to incentivize energy storage and thus are an important input for this method. Commercial utility electric rate structures often have peak-demand charges or time-of-use rates. Such rate structures encourage users to charge energy storage systems in less expensive periods and discharge the stored energy during more expensive periods. Demand charges commonly range from 10-30 USD/kW, though they can be as high as 90 USD/kW for commercial and industrial consumers [119] and are assessed using the maximum demand power, typically in the trailing 15-minute moving average of the metered load for some time period in a billing cycle (typically all time, an on-peak period during a monthly billing cycle, or a combination of both). Thus, the simulated total and thermal electric demand power profiles used to demonstrate this method use a 15-minute timestep.

The examples demonstrated in this thesis focus on the peak demand reduction potential of hybrid BES/TES systems, although this approach can also be used with TOU electricity rates. Therefore, the utility rate structure used for all results in this study includes a flat energy price of 0.12 USD/kWh and a demand charge assessed for all time in a monthly billing cycle of 15 USD/kW. The study also explores the impact of assessing demand charges on all months or only for the cooling season (May to September).

3.2. Energy storage system models

The proposed methodology uses simple storage models that do not represent specific energy storage systems but capture the overall trends, tradeoffs, and potential synergies of a hybrid BES/TES system. For example, the battery is not based on a particular chemistry, and the TES model is not based on a particular type or brand (e.g., ice tank, chiller, PCMs). The battery and thermal energy storage models are defined by a constant electrical round-trip efficiency and specified maximum allowed rate of discharge (as a C-rate). Future studies could extend this analysis by increasing the quality of storage modeling, such as by analyzing a particular battery chemistry or making the thermal energy storage round-trip efficiency a function of other variables like chiller type or ambient temperature.

3.2.1. Round-trip efficiencies for analyzed storage systems

Equation (3.1) defines the energy storage round-trip efficiency (η_{ES}) as the ratio between metered electrical energy avoided by the storage system and the electrical energy supplied to the storage system. The "avoided" energy, E_{avoided}, is the consumed energy that would have otherwise been met by the grid had the owner not discharged energy from the storage system. The "supplied" energy, E_{supplied}, is the electrical energy used during off-peak periods to charge the storage. This

term captures, for example, the electrical energy to the battery or electrical energy to the chillers which supply cool thermal energy to an ice tank.

$$\eta_{\mathrm{ES}} = \frac{E_{\mathrm{avoided}}}{E_{\mathrm{supplied}}} \tag{3.1}$$

The round-trip efficiency defined in Equation (3.1) is also equivalent to the battery's round-trip efficiency—the ratio between the electric energy available for discharge, $E_{\mathrm{discharge}}$, and the energy required to charge the battery, E_{charge}, as shown in Equation (3.2).

$$\eta_{\mathrm{BES}} = \frac{E_{\mathrm{discharge}}}{E_{\mathrm{charge}}} \tag{3.2}$$

Equation (3.3) defines the thermal round-trip efficiency of a TES, $\eta_{\mathrm{TES,th}}$, as the ratio of the thermal energy discharged to the thermal energy supplied during charging. This efficiency captures thermal energy losses, so its value is dependent on the duration of storage and other factors like ambient temperature.

$$\eta_{\mathrm{TES,th}} = \frac{Q_{\mathrm{discharge}}}{Q_{\mathrm{charge}}} \tag{3.3}$$

To compare with the battery round-trip efficiency, an equivalent electrical round-trip efficiency, η_{TES}, is defined in Equation (3.4). The avoided electrical energy is the difference between the electrical energy which would have been needed to meet the thermal load with baseline equipment, E_{base}, and meeting the thermal load by discharging from a TESS, $E_{\mathrm{discharge}}$.

$$\eta_{\mathrm{TES}} = \frac{E_{\mathrm{base}} - E_{\mathrm{discharge}}}{E_{\mathrm{charge}}} \tag{3.4}$$

Equation (3.4) can be expanded in terms of thermal energy and corresponding average Coefficients of Performance (COP), shown in Equation (3.5). The COP is the ratio of thermal energy output, Q, to electrical energy input, E. That is: $COP = Q/E$ or $E = Q/COP$.

$$\eta_{\text{TES}} = \frac{\frac{Q_{\text{base}}}{\overline{COP_{\text{base}}}} - \frac{Q_{\text{discharge}}}{\overline{COP_{\text{discharge}}}}}{\frac{Q_{\text{charge}}}{\overline{COP_{\text{charge}}}}} \tag{3.5}$$

Neglecting losses in transmission, both E_{base} and $E_{\text{discharge}}$ have the same quantity of thermal energy delivered to the zone (i.e., $Q_{\text{base}} = Q_{\text{discharge}}$). Factoring out the thermal loads, multiplying both the numerator and denominator by $\overline{COP_{\text{charge}}}$, and substituting the definition of the thermal round-trip efficiency, $\eta_{\text{TES,th}}$, yields Equation (3.6), which is useful since it relates terms typically associated with characterizing a thermal energy storage system (i.e., COP of charging, COP of discharging, thermal losses) in a form that is equivalent to the electrical round-trip efficiency of a battery. Thus, the two systems may be quickly compared for electrical energy shifting efficiency.

$$\eta_{\text{TES}} = \left(\frac{\overline{COP_{\text{charge}}}}{\overline{COP_{\text{base}}}} - \frac{\overline{COP_{\text{charge}}}}{\overline{COP_{\text{discharge}}}}\right)\eta_{\text{TES,th}} \tag{3.6}$$

Batteries' round-trip efficiencies are typically specified by the manufacturer and are commonly between 85-95% [7]. Thermal storage systems have a higher range of possible values, varying between 80-115%, because the expression depends on more variables, including condenser-side (ambient) and evaporator-side (zone) temperature dependence of COPs for charging and discharging, as well as thermal loss variables [120]. Thus, in this analysis, we assume both energy storage systems have constant electrical round-trip efficiencies of 90%.

The electrical round-trip efficiency of a hybrid system is calculated using a weighted average of its components' efficiencies, Equation (3.7):

$$\eta_{\text{HES}} = \beta\, \eta_{\text{BES}} + \tau\, \eta_{\text{TES}}, \tag{3.7}$$

where β is the fraction of discharge energy contributed by the BES, and τ is the fraction of discharge energy contributed by the TES.

3.2.2. Discharge energy capacity and maximum C-rates for analyzed storage systems

The discharge C-rate is the ratio of power of discharge and the nominal discharge energy capacity. For example, a discharge rate of 1C will deplete the storage in 1 hour, while 2C depletes the storage system in 0.5 hours. Thus, in this study, the discharge power capacity is calculated as the discharge energy capacity divided by the maximum C-rate.

In any simulation, the highest possible discharge rate is the discharge power that results in the system being fully depleted in one timestep, since discharge must be uniform during the entire timestep. Therefore, 4C is maximum possible discharge C-rate for simulations presented in this study, which use 15-minute timesteps. Additional constraints to the discharge rate may be imposed for either system in this model. Here, the battery discharge is limited to 1C while the TES remains free to discharge at up to 4C. Although 4C may seem unrealistic for TES, this approach prioritizes TES over BES. With such prioritizing, high C-rates are only seen for storage systems with relatively small discharge energy capacities.

3.2.3. System lifetime and capital costs

For annual analysis, Section 4.3.3 describes a basic approach for estimating the user's total annualized cost savings resulting from utilizing the storage system after accounting for the lifetime of the device and capital expenses. Although this is a preliminary investigation, the analysis still gives insight into general trends associated with relative storage system costs and their ability to shift different kinds of loads at different times of year. A rigorous techno-economic analysis of a hybrid energy storage system could account for many factors such as utility costs, rates of storage charging and discharging, cycling and degradation behavior, opportunity costs, interest rates, external incentives and subsidies, and present and predicted future capital costs (among many others) playing a role in determining the optimal size and dispatch strategy from an economics

perspective. This study avoids such complexities and simply uses a constant lifetime and a single term for capital cost per unit of discharge energy capacity (or avoided electrical energy) in the proposed simplified annualized analysis. See Section 4.3.3 for more details on the annualizing assumptions and capital costs used for the examples in this study.

3.3. Electric demand power profile

While the proposed method can use measured data, this thesis analyzes simulated electric demand power profiles for different scenarios combining a building with EV charging stations and/or PV generation. The following sections describe how the building total and thermal load, PV generation, and EV load profiles are obtained. Specifically, four scenarios are investigated:

1) Building: Baseline building with no PV and no EV charging
2) Building+PV: Building with 600 kW of rooftop PV and no EV charging
3) Building+EV: Building with no PV and 6 EV charging stations
4) Building+PV+EV: Building with 600 kW of rooftop PV and 6 EV charging stations

3.3.1. Building energy model

This study uses an EnergyPlus model for a big-box grocery and retail store, which was calibrated to data from a store in Centennial, CO as provided by NREL. This calibrated model is simulated using EnergyPlus Version 9.3.0 and typical meteorological year (TMY3) data for the Sky Harbor International Airport in Phoenix, AZ. Phoenix was selected due to its high average temperatures and long cooling season, which translates to higher potential for TES utilization. However, the proposed methodology could apply to other building types and climate zones. The annual load profile, along with the load profile for the peak summer day, is shown in Figure 3.2.

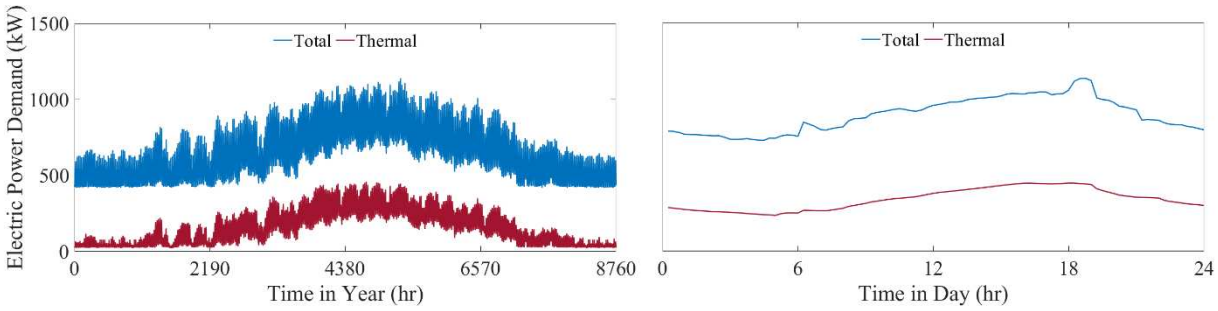

(a) (b)

Figure 3.2: Baseline building total and thermal electric demand power profiles for (a) the entire year and (b) the peak summer day

3.3.2. EV charging model

This study uses an EV charging profile based on a relatively aggressive transition to EVs nationwide. The EV profile was provided by NREL and generated using EV-EnSite, which is a direct current fast charging (DCFC) model based on EVI-Pro. Further detail is available in the literature [121]–[123]. This study uses a 350-kW charging rate and 6 charging stations on the same meter as the building. Each station has 16 events per day. The events are 5-15 minutes long depending on the state of charge of the vehicle when it arrives at the station. The annual EV load profile along with the profile for a typical summer day are shown in Figure 3.3.

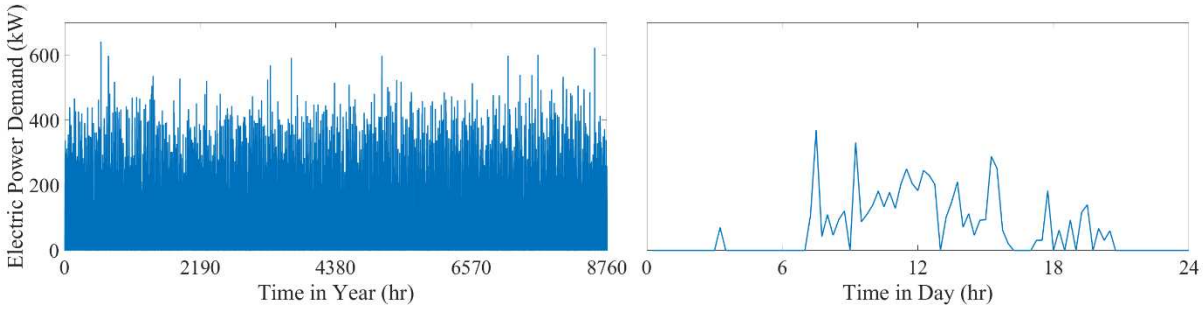

(a) (b)

Figure 3.3: Electric demand power associated with EV charging for (a) entire year and (b) a typical summer day

3.3.3. PV generation

PV generation profiles are simulated using the "Detailed PV Model" in NREL's System Advisory Model (SAM), Version 2020.2.29 Rev. 2 and the same weather data as the building model. The resulting generation profile is scaled so that the peak power provided by the PV array is 600 kW. Cubic spline interpolation is applied to increase the resolution from 1-hour timesteps to 15-minute timesteps. Figure 3.4 shows the annual PV generation profile and the profile for three example days.

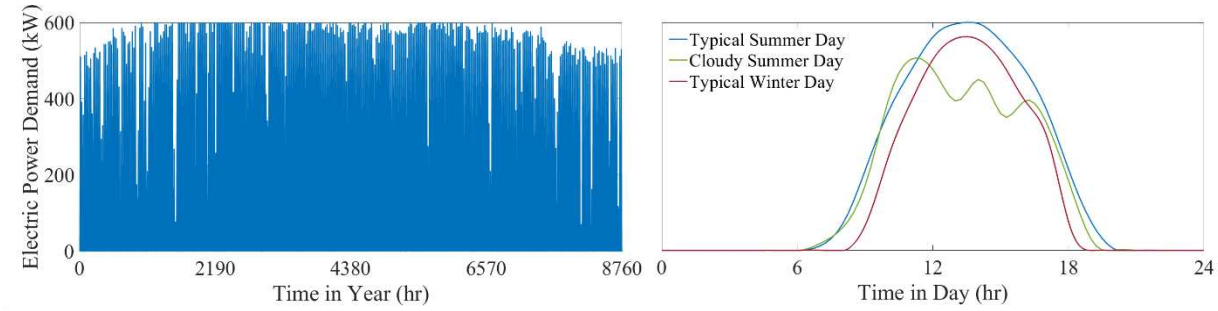

(a) (b)

Figure 3.4: Normalized PV Generation for Phoenix, AZ using "Detailed PV Model" in SAM; (a) entire year and (b) example days

This chapter introduced the analytical method model inputs, including the variable utility rate structure, energy storage system models, and the total and thermal electric load profiles. For the demonstration scenarios used in this study, the load profiles are combinations of a simulated big-box grocery and retail building, EV charging, and PV. The following chapter describes the analytical method in more detail, including a description of the binary search approach and the sizing and dispatch algorithms.

CHAPTER 4

ANALYTICAL METHODS FOR SIZING AND IDEALIZED DISPATCH

This chapter describes the new analytical method in detail, as outlined in Figure 4.1. Section 4.1 introduces constraints imposed to ensure the energy storage shifting always yields electricity cost savings, depending on the utility rate structure. Section 4.2.1 explains how a binary search method is applied for the two algorithms which determine (Section 4.2.2) sizing or (Section 4.2.3) idealized dispatch of a given hybrid energy storage system. Post-processing steps such as calculating annual utility cost savings or annualized total cost savings are presented in Section 4.3. Finally, Section 4.4. discusses how load duration curves are used to visualize results.

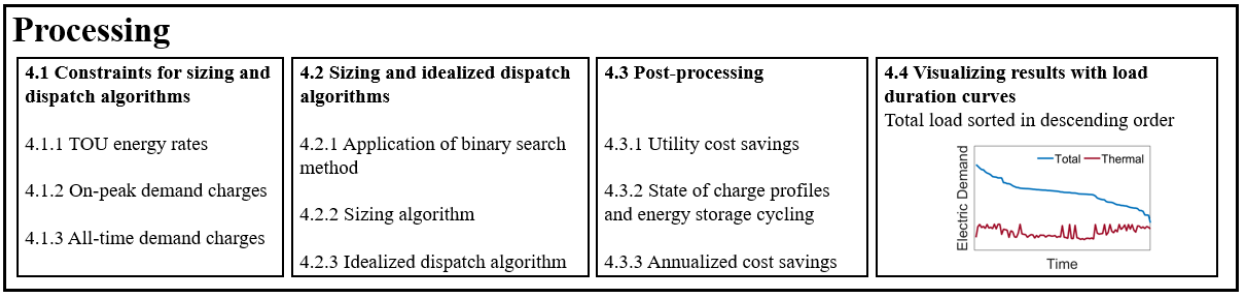

Figure 4.1: Outline of constraints and procedures in the proposed analytical sizing and dispatch approach for energy storage systems

4.1. Constraints on maximum potential energy shifting or demand shaving

This thesis focuses on electricity cost savings resulting from energy shifting or demand shaving. This section explores constraints on the utilization of storage that result from the requirement that energy storage results in a reduction of electricity costs. Constraints and other considerations are broken down by the rate structure. Section 4.1.1 is concerned with time-of-use rates, Section 4.1.2 discusses demand charges assessed for an on-peak period, and 4.1.3 elaborates on demand charges assessed for all time during the billing cycle.

4.1.1. Time-of-use energy rates

For utility rate structures composed of only TOU rates without demand charges, the electricity cost savings obtained from energy storage depends on the TOU ratio, storage efficiency, and quantity of energy shifted. To ensure storage produces electricity cost savings, the electricity cost required during charging must be less than the cost of avoided energy during discharging. This inequality is shown in Equation (4.1):

$$p_{\mathrm{L}}\, E_{\mathrm{supplied}} < p_{\mathrm{H}}\, E_{\mathrm{avoided}} \tag{4.1}$$

where E_{supplied} and E_{avoided} are the energy supplied during charging and the energy avoided during discharging, respectively. p_{L} and p_{H} are the low (off-peak) and high (on-peak) energy prices, respectively. Using the definition of the round-trip efficiency shown in Equation (3.1), Equation (4.1) can be rearranged—Equation (4.2)—and simply expresses that the round-trip efficiency must be greater than a ratio of energy rates:

$$\frac{p_{\mathrm{L}}}{p_{\mathrm{H}}} < \eta_{\mathrm{ES}} \tag{4.2}$$

Thus, regardless of the nominal discharge energy or discharge power capacities of the storage system, energy storage certainly cannot be profitably utilized under a rate structure of only TOU energy rates if the round-trip efficiency of storage does not exceed the inverse of the TOU ratio. If the storage's round-trip efficiency satisfies Equation (4.2), full shifting is the maximum possible shifting that can be accomplished. Figure 4.2 shows the maximum energy discharge for a TOU rate structure for three different energy storage systems.

a) Frame 1 shows that, for a battery, the maximum amount of energy that can possibly be shifted by the battery and still result in electricity cost savings is limited only by the amount of energy that would have otherwise been supplied by the grid during the on-

peak period. This is equal to the area, highlighted in yellow, under the total electric demand power curve during the on-peak period.

b) Frame 2 shows that thermal storage is only useful when there is a thermal load. In most US climates, there is at least some thermal load in commercial buildings during operating hours. The maximum amount of energy that can possibly be shifted using TES is equal to the area, highlighted in red, under the thermal electric demand power during the TOU period. This is the energy that would have been required to meet the thermal load using baseline equipment during on-peak hours.

c) Frame 3 shows that full shifting can be accomplished by a hybrid system, as long as the hybrid system's battery has sufficient energy and power capacity to handle the nonthermal loads inaccessible to the TES.

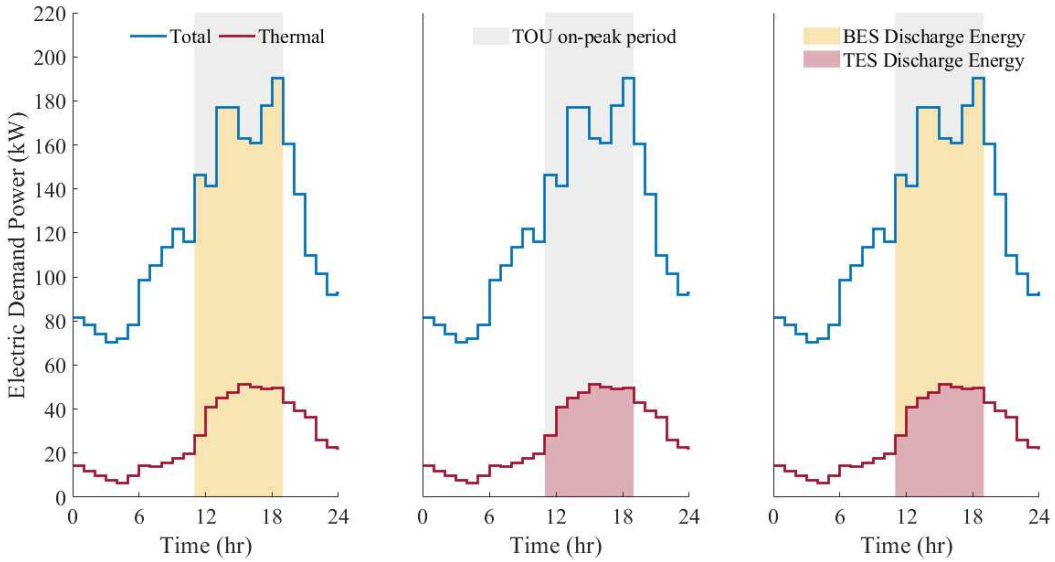

Figure 4.2: Maximum possible energy shifting under a TOU rate for BES (Frame 1), TES (Frame 2), or HES (Frame 3); figure shows an arbitrary load profile for a single day with an on-peak period occurring from 11:00 A.M - 7:00 P.M. Full shifting occurs when either the total electric demand power (Frames 1 and 3) or the thermal electric demand power (Frame 2) is reduced to zero by storage discharge during the on-peak period

4.1.2. Demand charges assessed for on-peak period in billing cycle

Demand charges can apply to all time in the billing cycle or to a specified on-peak period. To assess the potential electricity cost savings associated with storage utilized to lower peak demand charges assessed for an on-peak period, this analysis considers incremental increases in discharge energy. Incrementally increasing the storage system's discharge energy capacity is useful as long as the cost of electrical energy avoided during storage discharge is greater than the cost of electrical energy that supplies the storage during charging. For cases with a demand charge, the inequality expressed in Equation (4.3) must be satisfied:

$$p_{\mathrm{E}}\Delta E_{\mathrm{charge}} < p_{\mathrm{D}}\Delta d + p_{\mathrm{E}}\Delta E_{\mathrm{discharge}} \tag{4.3}$$

where p_{E} is the flat price for energy, p_{D} is the demand charge, Δd is the reduction in peak total electric demand power, and $\Delta E_{\mathrm{discharge}}$ is the incrementally increased amount of discharging energy which requires an incremental amount of additional charging, $\Delta E_{\mathrm{charge}}$. In the case of discharging stored energy, the incremental unit of discharged energy, $\Delta E_{\mathrm{discharge}}$, will reduce the electricity cost of energy during the on-peak period by an amount $p_{\mathrm{E}}\Delta E_{\mathrm{discharge}}$ and will reduce the demand charge by an amount $p_{\mathrm{D}}\Delta d$, as shown in Figure 4.3. The reduction in demand power, Δd, is related to the incremental discharge energy, $\Delta E_{\mathrm{discharge}}$, by Equation (4.4):

$$\Delta d = \frac{\Delta E_{\mathrm{discharge}}}{t_{\mathrm{shave}}} \tag{4.4}$$

Equation (4.4) and Figure 4.3 show that the ability of incremental increases in discharge energy to further reduce peak demand by incremental values of Δd will gradually be diminished as t_{shave}, the sum of discharging timesteps, increases.

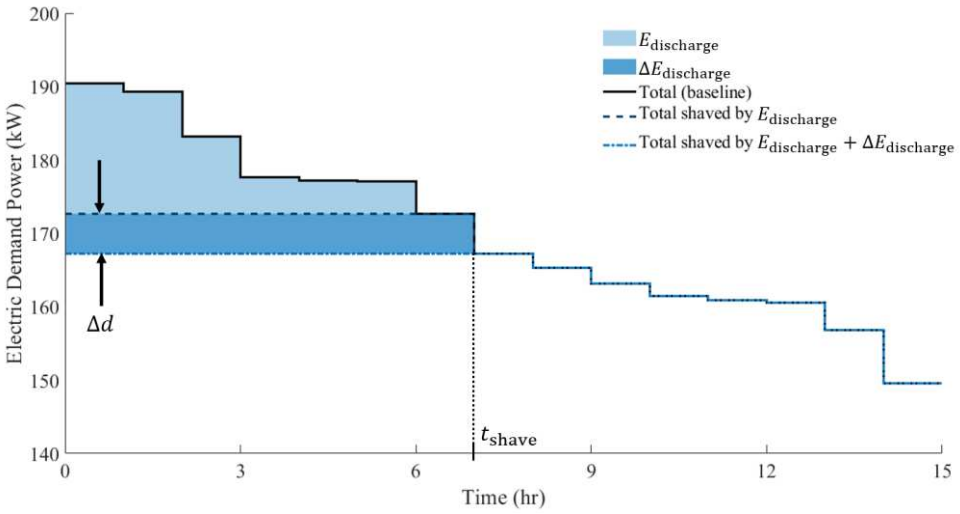

Figure 4.3: Relationship between the incremental increase in discharge energy and incremental demand reduction

In Equation (4.5), the charge and discharge energy are related using η_{ES}:

$$p_{\text{E}} \frac{\Delta E_{\text{discharge}}}{\eta_{\text{ES}}} < \left(\frac{p_{\text{D}}}{t_{\text{shave}}} + p_{\text{E}} \right) \Delta E_{\text{discharge}} \tag{4.5}$$

Dividing out the discharge energy and solving for the energy storage round-trip efficiency reveals that incremental increases in storage will continue to provide electricity cost savings until the discharge energy's effect on demand reduction is diluted such that $t_{\text{shave,max}}$ makes the following true:

$$\frac{p_{\text{E}}}{\frac{p_{\text{D}}}{t_{\text{shave,max}}} + p_{\text{E}}} = \eta_{\text{ES}} \tag{4.6}$$

The maximum time of shaving, $t_{\text{shave,max}}$, defines the maximum number of timesteps for which discharging energy is certain to result in electricity cost savings, given a storage's round-trip efficiency, the price of the demand charge, and flat energy costs.

For all three energy storage types analyzed in this study (BES, TES, and hybrid), the maximum possible peak demand reduction depends on the magnitude of the maximum time of shaving. If $t_{\text{shave,max}}$ is less than the on-peak time period, the maximum shaving is calculated as

shown in Figure 4.3, where t_{shave} in the figure equals $t_{\text{shave,max}}$. Alternatively, if the maximum time of shaving is greater than or equal to the length of the on-peak time period, then the maximum possible peak demand reduction is limited only by the system's ability to reduce demand in the on-peak window, illustrated in Figure 4.4 (following page).

a) For a battery, this occurs with full shifting, so that the maximum demand reduction, Δd, is equal to the maximum total electric demand power in the on-peak period, as shown in Figure 4.4 Frame 1.

b) Frame 2 shows peak shaving by TES. The peak demand is reduced by avoiding using baseline equipment until some timestep has no thermal electric demand power.

c) Just as with TOU energy rates, the maximum reduction for a hybrid system is the same as the battery, as long as the battery is sufficiently large. Notice that TES utilization can potentially increase as a result of adding a battery (compare TES utilization in Frame 2 and Frame 3). A hybrid system may achieve the same peak demand reduction as a BES-only case with a battery of a smaller discharge energy capacity in a hybrid system when the remaining discharge is handled by the TES.

4.1.3. Demand charges assessed for all time in billing cycle

For demand charges which are assessed at all time in the billing cycle, the relationships between maximum time of shaving, the rate structure, and the round-trip efficiency are the same as for on-peak demand charges. However, the maximum possible shaving is also limited by load flattening. The load is flattened when the metered demand power is constant for the duration of storage, which occurs when storage discharge shaves all peaks and storage charging fills all valleys. At this constant demand power, any further charging of the storage will cause the demand power during charging timesteps to exceed the load-shaved demand power during discharging

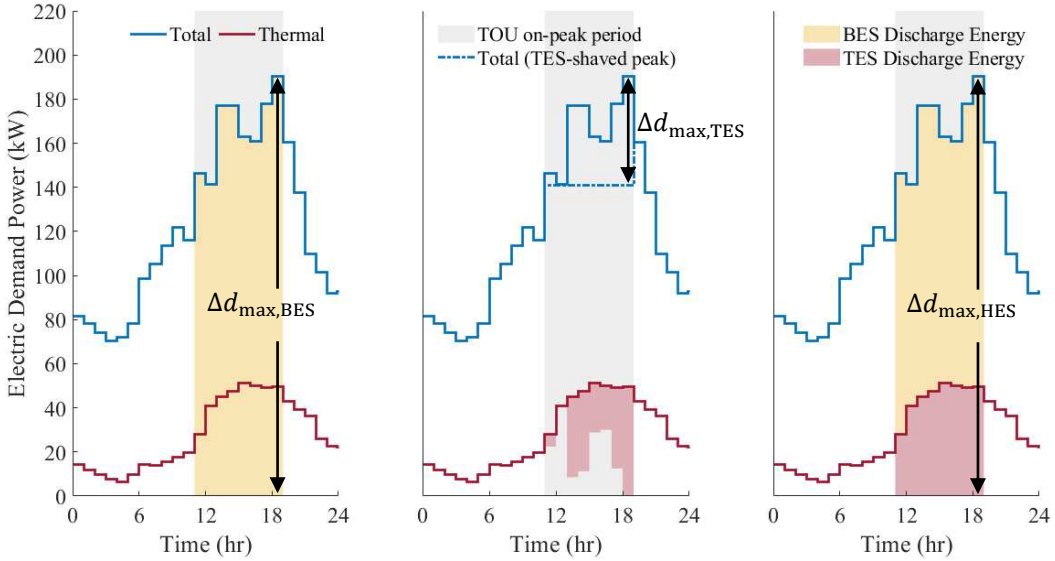

Figure 4.4: Maximum possible peak shaving for an on-peak demand charge for different system types. Frame 1 shows BES-only, Frame 2 shows TES-only, and Frame 3 shows a hybrid system

timesteps. Thus, demand power during charging will become the new peak and will cause the discharge times to become the new valley. Load flattening should be calculated such that the demand power is constant during any period of the length of the storage, which in this study is 24 hours. Figure 4.5 shows the load flattening and maximum demand reduction potential for the three system types.

a) In this figure, the battery efficiency is low. Frame 1 shows how load flattening occurs around 140 kW, where significantly more charging energy is required for a relatively small amount of discharge due to the low BES efficiency.

b) In Frame 2, TES achieves about the same maximum demand reduction as with the BES; however, the limiting factor is the existence of a thermal load. The shaved load shown in the dashed red line reaches zero around 18 hours. Less charging is required than for the BES-only case since the TES efficiency is greater.

c) Frame 3 shows a hybrid system. In this case, TES utilization increases, since TES discharge accounts for BES discharge assisting on timesteps where the thermal electric load has been eliminated. Thus, although the BES efficiency is very low, greater peak shaving is achieved in the hybrid system.

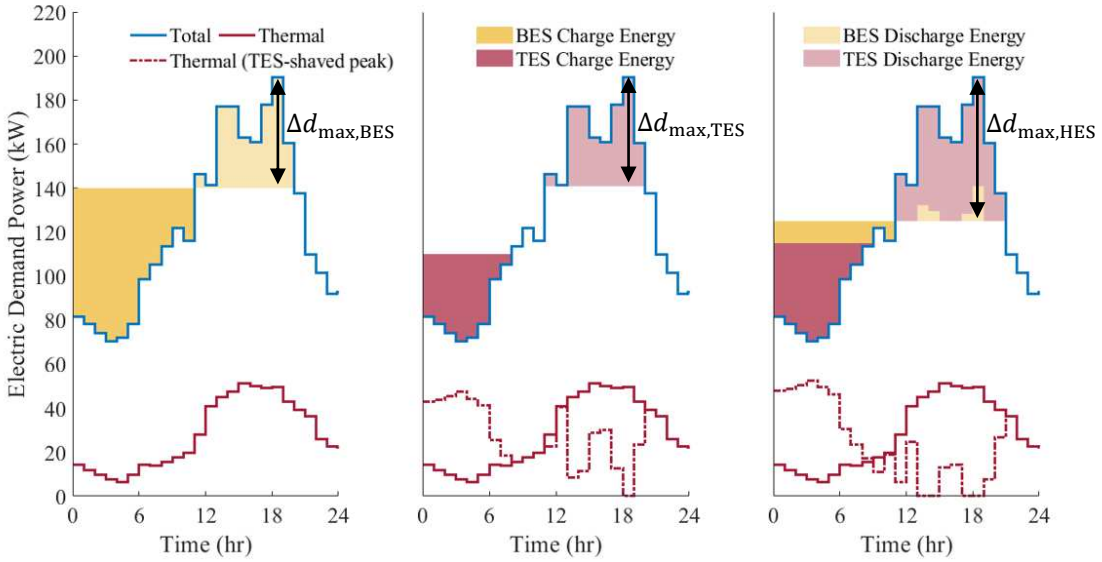

Figure 4.5: Maximum possible peak shaving for an all-time demand charge for different system types. Frame 1 shows BES-only, Frame 2 shows TES-only, and Frame 3 shows a hybrid system

4.2. Sizing and idealized dispatch algorithms

This thesis features two algorithms which calculate (1) the energy and power requirements needed to achieve an arbitrary target amount of peak demand reduction, and (2) the idealized dispatch strategy which will yield the maximum peak shaving potential of different combinations of batteries and/or thermal energy storage for months with a demand charge. Both algorithms utilize a binary search approach.

4.2.1. Binary search approach

In a binary search, a solution is known to exist between an upper and lower bound. The solver will update guesses, reducing the range of the bounds by half each time, until the solution

is obtained. In this problem, the "solution" is the value of electric demand power after shaving has reduced peak demand as much as possible. Meanwhile the initial bounds depend on the utility rate structure. For on-peak period rate structures, full shifting is possible; therefore, the bounds for the binary search are the maximum load and zero. For demand charges assessed at all times in the billing cycle, the minimum peak demand occurs when the load is flattened; thus, the initial bounds are the maximum and minimum load.

The binary search for the minimized peak demand power is illustrated in Figure 4.6. Frames 1-4 show how the storage-shifted load profile is calculated for a given guess. The solid blue stair profile is a total electric demand power profile for some arbitrary building. The solid black line represents the current guess. Starting with the first timestep in which discharge of stored energy is required (i.e., the load exceeds the guess), the solver identifies the energy and power required to shave the load to the guess and increases the load to charge storage during off-peak times in the preceding 24 hours (Frame 2). The light-red area is the energy avoided by utilizing TES, while the light-yellow area shows the energy avoided by utilizing BES. The current algorithm uses a valley filling approach for charging, though this could be improved depending on the objective. For example, charging could prioritize timesteps with the most favorable COP or seek to charge the storage as uniformly as possible (i.e., constant electric power supplied to storage). In these algorithms, TES is prioritized, but it is still inherently limited by the presence of a thermal load. Frame 3 shows the process continuing while Frame 4 shows the final discharge timestep being accounted for. After accounting for all required charging needed to discharge the storage system during discharge timesteps, Frame 4 shows the resulting storage-shifted load profile in a dashed blue line (and Frame 5 shows the same case, but without highlighting the final discharging timestep with unique colors).

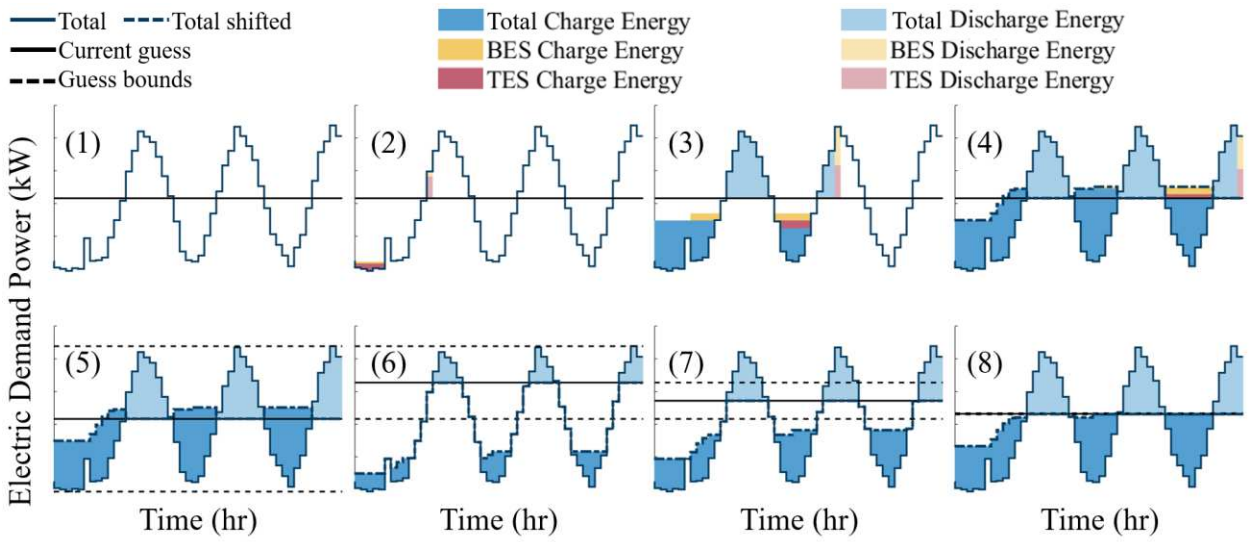

Figure 4.6: Visual representation of discharging/charging strategy for a given guess (Frames 1-4) and updating guess in binary search (Frames 5-8)

In the case of the guess value used in Frames 1-4, the shifted load profile exceeds the guess value. Thus, the specified storage system(s) are unable to shave the load to the guess value. Frame 6 shows the updated guess in which less shaving occurs. Note that the updated guess is half-way between the same upper bound and the previous guess. In Frame 6, the shifted load never reaches the guess value, indicating that more shaving is possible. Therefore, in Frame 7, the guessed amount of shaving is increased. This continues until the solution is obtained to within the desired tolerance, as shown in Frame 8.

4.2.2. Sizing algorithm to obtain minimum energy and power requirements for target peak shaving

A. Determine maximum possible demand reduction: The maximum monthly peak shaving is calculated using the binary search approach just described. Note that the algorithm will also confirm that utility cost savings are obtained by decreasing the guessed amount of peak shaving if the time of shaving (i.e., sum of all discharging timesteps) exceeds the maximum allowed time of shaving, $t_{\text{shave,max}}$, as determined in Section 4.1.1.

B. Sweep through range of possible values of target peak demand reduction: Using the maximum possible peak demand reduction identified in Step A, Steps C-E are repeated for a range of values of target peak demand reduction between zero and the maximum shaving.

C. Determine BES energy and power capacities: The BES is sized first by summing the nonthermal loads that exceed the target value of peak demand power for each day in the month. The BES is sized first (and independently of the TES) since nonthermal loads cannot be met by TES. This sizing assumes that the storage system discharge capacity is high enough to deliver all required discharge energy in a day with one full depth of discharge. In some cases, recharging may be possible (such as if there is significant PV creating a "bimodal" profile), and the required minimum energy capacity could be calculated to account for such cycling. The required BES power capacity is equal to the timestep with the highest nonthermal load above the target peak shaving.

D. Determine TES energy capacity based on BES energy capacity: Although the BES is sized independently of the TES, the minimum required TES depends on the BES capacity. This is because the BES may be useful for meeting loads that the TES meets (e.g., the battery is used to run a chiller), whereas the TES cannot always meet BES loads (e.g., the chiller cannot deliver power for plug loads). Therefore, the TES is sized by finding the day with the maximum required energy of discharge and subtracting the BES capacity calculated in Step B.

E. Update energy capacities to satisfy C-rate limit: The discharge C-rate for each energy storage system is determined using the power and energy capacities calculated in the previous steps. If the calculated C-rate exceeds the physical C-rate limit (imposed as a

model input, see Section 3.2.2), the energy capacity is increased such that the calculated C-rate is equal to the C-rate limit.

4.2.3. Peak shaving potential for different combinations of BES and TES

The second algorithm views the problem from the opposite perspective. Instead of assuming a target amount of peak demand reduction and determining what combination of energy storage assets are required to achieve that peak shaving, it determines what peak shaving is possible given varying sizes of TES and battery storage.

A. Determine the range of battery and TES capacities to analyze: In theory, any size of energy storage system could be defined and analyzed with this algorithm. To specify an upper bound of system capacities to analyze, the first algorithm is repeated for each month in the year. The month with the maximum useful battery is used to set the upper bound of systems analyzed.

B. System selection: A nested four-part for loop cycles through every combination of energy and power capacities for both components in the hybrid system to be analyzed. Step C is repeated for each combination.

C. Determine the peak demand reduction for each month in the year, for the given storage system: The maximum possible peak demand reduction is calculated for each month with a demand charge for the given storage system. The demand reduction is calculated using the binary search method described in 4.2.1, where the guessed amount of peak shaving is increased until none of the required power and energy capacities (discharging for total electric loads above the guess) exceed the specified system's capacities.

4.3. Post-processing

After calculating the potential peak reduction for each month, the algorithm output is processed to obtain demand charge/utility cost savings, annual equivalent full cycles of the battery, and annualized cost savings (accounting for annualized capital costs of the storage system). These metrics taken together are used to identify tradeoffs and synergies of hybrid storage systems.

4.3.1. Utility cost savings

The total energy bill the customer pays is comprised of demand charges and energy costs. The portion of the energy costs associated with demand charges (in USD/kW) is reduced by dispatching the storage system. However, the contribution to the total bill associated with the energy costs (in USD/kWh) increases due to energy losses, since the round-trip efficiencies of either component are less than 100%. The annual utility cost savings, UCS, may be expressed as:

$$UCS = (\sum_{m=1}^{12} PS_m) p_{\mathrm{D}} - E_{\mathrm{discharge}} \left(\frac{1}{\eta_{\mathrm{HES}}} - 1\right) p_{\mathrm{E}} \tag{4.7}$$

where PS_m is the peak shaved in month m, p_{D} is the demand charge in USD/kW, $E_{\mathrm{discharge}}$ is the total energy of discharge over the year for the battery and thermal energy storage system in $\mathrm{kWh_e}$, and p_{E} is the flat energy rate in USD/kWh. If the demand charges are only assessed for summer months, the above equation (which sums over 12 months) still holds, since PS_m will be 0 kW for months without a demand charge.

4.3.2. State of charge profile and annual battery cycling

After calculating the timesteps for discharge and charge in the final solution, the state of charge (SOC) of the storage system is constructed. Having the SOC over the full year would allow calculation of cycles using more sophisticated methods like rain-flow cycle counting. In this study, however, the battery cycling is characterized by the simpler annual equivalent full cycles (EFC) method, which sums all discharge over the year, $E_{\mathrm{BES,discharge}}$, and divides by the nominal

capacity. For example, four consecutive days with 25% of a full depth of discharge would be counted as one equivalent full cycle.

4.3.3. Annualized cost savings

The annualized cost savings are calculated by subtracting annualized energy storage costs from the annual utility cost savings, using Equation (4.8):

$$ACS = UCS - ACC_{\mathrm{ES}} \tag{4.8}$$

In Equation (4.8), the annualized capital cost of the energy storage system, ACC_{ES}, is a function of the total capital cost of the device, the discount rate, and the lifetime of the storage. This is calculated using the same method found in existing studies ([11], [124]) as:

$$ACC_{\mathrm{ES}} = CC_{\mathrm{ES}} \frac{r}{1-\frac{1}{(1+r)^{l_{\mathrm{ES}}}}} \tag{4.9}$$

where CC_{ES} is the total capital cost of the energy storage system device, r is the discount rate, and l_{ES} is the lifetime of the energy storage. For this study, the lifetime is treated as a constant, though future studies could improve by making the lifetime dependent on other factors, such as annual cycling. The capital cost of the device is specified using a total discharge energy capacity, and a cost per unit discharge energy capacity, which can vary depending on the C-rate.

Table 4.1 shows the parameters used for annualizing the capital expense of the energy storage. The battery cost in USD/kWh$_e$ includes all balance of plant and installation costs for a 1-hour duration (i.e., 1C) battery [125]. Two TES costs are used. 100 USD/kWh$_e$ is the average cost of existing chiller projects (including installation costs), in USD/kWh$_{th}$, scaled by a presumed COP of 3.14 to correspond to USD/kWh$_e$ [124], and 600 USD/kWh$_e$ is equal to the capital cost for BES. These two values are used to explore the value of hybrid systems when TES is significantly cheaper than BES (often the case) or if the two systems cost the same (worst-case scenario for TES utilization).

Table 4.1: Parameters Used to Calculate the Annual Cost Savings of Energy Storage

Parameter	Value
Discount rate, r (%)	8
TES system lifetime, l_{TES} (years)	15
BES system lifetime, l_{BES} (years)	15
Demand charge, p_{D} (USD/kW)	15
Demand periods	January-December or only May-September
Capital cost including all balance of plant (USD/kWh$_e$)	Battery: 600 Thermal energy storage: 600 or 100

4.4. Visualizing results with load duration curves

A load duration curve sorts the electric load profile in descending order. It is termed "duration" because one can use it to identify the number of hours for which the load is at or above a specific value. Although use of load duration curves is common in grid-side analysis (where different durations of the load at different power correspond to the applicability of different generation resources), their use within meter-side analysis is less common.

The load duration curves used here are based on the total electric demand power for the scenario and the electric demand power associated with thermal loads of space cooling the retail building. The thermal load is sorted in the same order as the total load, so that the thermal profile is not necessarily descending, but instead shows the coincident thermal load with the sorted total electric demand.

Figure 4.7 shows a monthly total and thermal electric load profile for a building and the corresponding load duration curve. These load duration curves give insight into peak shaving potential for energy storage systems that are composed of some combination of batteries and thermal energy storage. In particular, the two curves (total and thermal) correspond to the applicability of the two types of energy storage considered—the battery can operate on any electric load (blue) while TES can shift electric loads associated with a thermal load (red). Subtracting the thermal load from the total load shows how nonthermal loads vary with the total load. An idealized

TES requiring no electricity input to discharge stored thermal energy can only shave thermal loads; thus, the maximum value of nonthermal loads (highest point on yellow curve) represents the lowest value to which TES can shave the total peak demand for a given month.

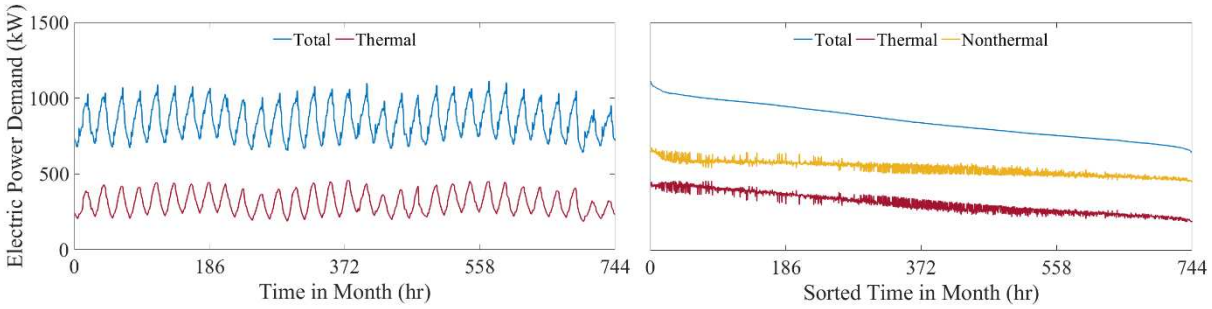

(a) (b)

Figure 4.7: Constructing a load duration curve; (a) shows the time-ordered total (blue) and thermal (red) load profiles for one month; (b) shows the load duration curve (blue), and the coincident thermal (red) and nonthermal (yellow) loads for the month

CHAPTER 5

RESULTS

The results of this study are divided in three parts: 1) load duration curves for each scenario, 2) the required battery and TES capacities for a desired peak load reduction using the first algorithm, and 3) the impact of battery and TES sizing using the second algorithm. The third part looks at potential synergies by calculating utility cost savings, equivalent full cycles for the battery, and an estimate for the total cost savings, including annualized capital costs.

5.1. Load profiles and load duration curves

Figure 5.1 shows the electric load profile for the entire year (Figure 5.1(a)) and for a summer day (Figure 5.1(b)) for each scenario: building (Base, blue line), building with PV (Base+PV, red line), building with EV charging (Base+EV, yellow line) and building with PV and EV charging (Base P+EV, purple line).

The day (June 19) in Figure 5.1(b) reaches the highest peak demand for the Building+EV scenario. The baseline building peaks in the evening due to increased air conditioning loads in the hot part of the day. EVs introduce significant variability to the load profile, with increases in demand of up to 500 kW over 15- to 30-minute durations. Rooftop PV reduces the building profile during daytime, lowering the day's peak by 7% and shifting it to later in the day. This also increases the ramp rate to ~175 kW/hr for the evening hours as the PV production declines and electric demand remains high. Including both EV and PV shows how significantly varied the load can be when metered-load reducing assets (e.g., PV) are combined with metered-load increasing assets (e.g., EV).

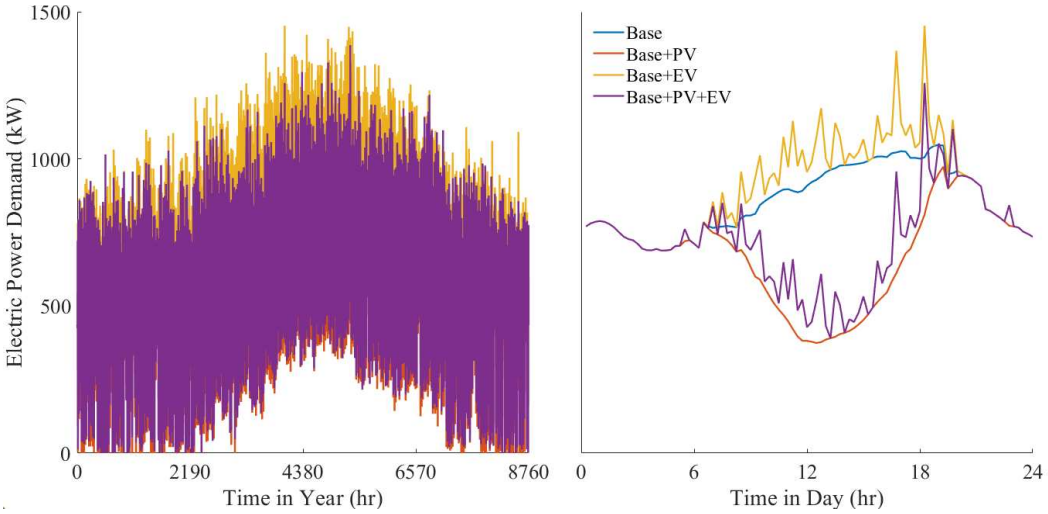

(a) (b)

Figure 5.1: (a) Annual electric load profiles for the four or the baseline building (Base), building with 600kW PV rooftop system (Building+PV), building with 6 EV charging stations (Building+EV) and building with PV and EV charging station (Building+PV+EV) and (b) daily electric load profile for July day for same four cases.

Load duration curves (Figure 5.2) make this visual comparison simpler than time-series data due to the sorting from highest to lowest. The inset figure on top right on Figure 5.2 shows the first 144 hours of the duration curve, which corresponds to the annual peak demand for each scenario. The peak demand for the baseline building is 1,100 kW. Adding fast-charge EVs increases this peak demand by 318 kW (28%), while adding PV reduces it by 33 kW (3%). The reduction in the peak by adding PV is limited because the peak PV generation is not coincident with the peak building demand. Similarly, adding PV to the Building+EV scenario reduces peak demand by 66 kW (5%), again due to the noncoincident nature of PV and the random nature of the EV charging. Although charging does happen during operating hours for the big-box retailer, the peak EV load (Figure 5.1(b)) does not coincide with the peak solar output (around noon) nor at the time of maximum thermal load (around 1500 hours).

Because the load duration curve is sorted from highest to lowest, an individual timestep plotted for one scenario (e.g., Building only) on the load duration curve may not align with the

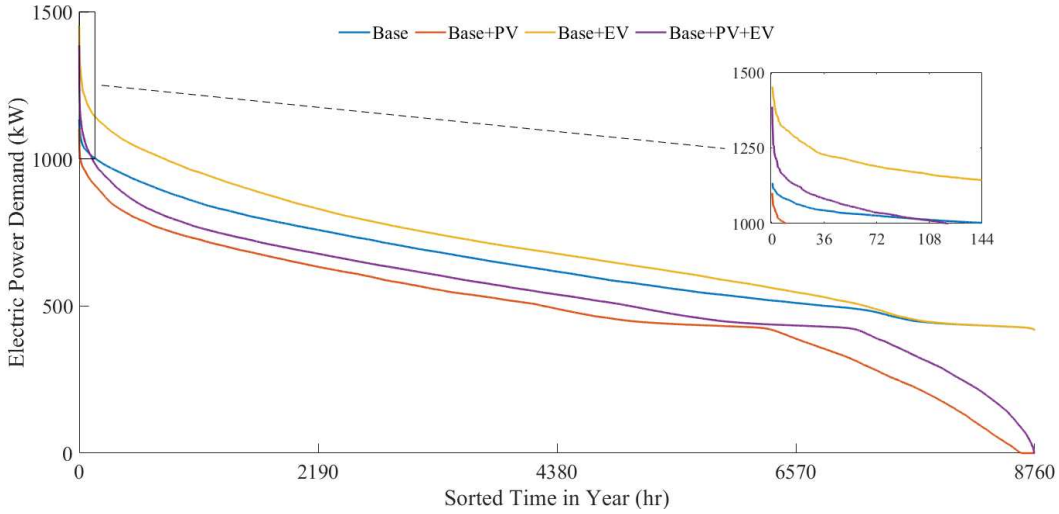

Figure 5.2: Annual load duration curve for the four scenarios; zoomed insert figure on top right shows the first 144 hours of the duration curve

same timestep for a different scenario (e.g., Building+ EV). For example, the "tail" seen at the last 20% of the load duration curve for the two scenarios with PV are typically from timesteps that were previously closer to the peak or "neck" (left end) of the baseline building curve.

Figures 5.3 and 5.4 (Pages 54 and 55, respectively) show the load duration curves for July and January along with the thermal and nonthermal load profiles for each of the four scenarios ((a)-(d)). The curves showing thermal electric demand power in each monthly load duration curve appear slightly differently since each building has a different total load duration curve. For the baseline building, the air conditioning load in January is only 13% of the total peak electric load, whereas in July it is 40% of the total peak electric load. This ratio depends on local weather and building type but shows a well-known trend: higher cooling electricity loads occur in summer due to higher temperatures and more mechanical cooling. When adding extreme-fast EV charging, the role of the cooling load on the peak demand is reduced to 4% and 29%, respectively.

In Figure 5.3(a) for the baseline building in summer, the thermal load is strongly correlated with the total load, with these two curves being relatively "parallel." This indicates that the nonthermal loads are relatively constant (yellow curve is relatively flat at 500-700 kW). In contrast,

Figure 5.4(d) shows that for the building with EV+PV in winter months, the thermal load is not strongly correlated to the total load. The nonthermal load increases at different timesteps by EV charging and is reduced at other timesteps by PV. The range of nonthermal loads as shown in yellow in Figure 5.4(d) is close to 0-1000 kW.

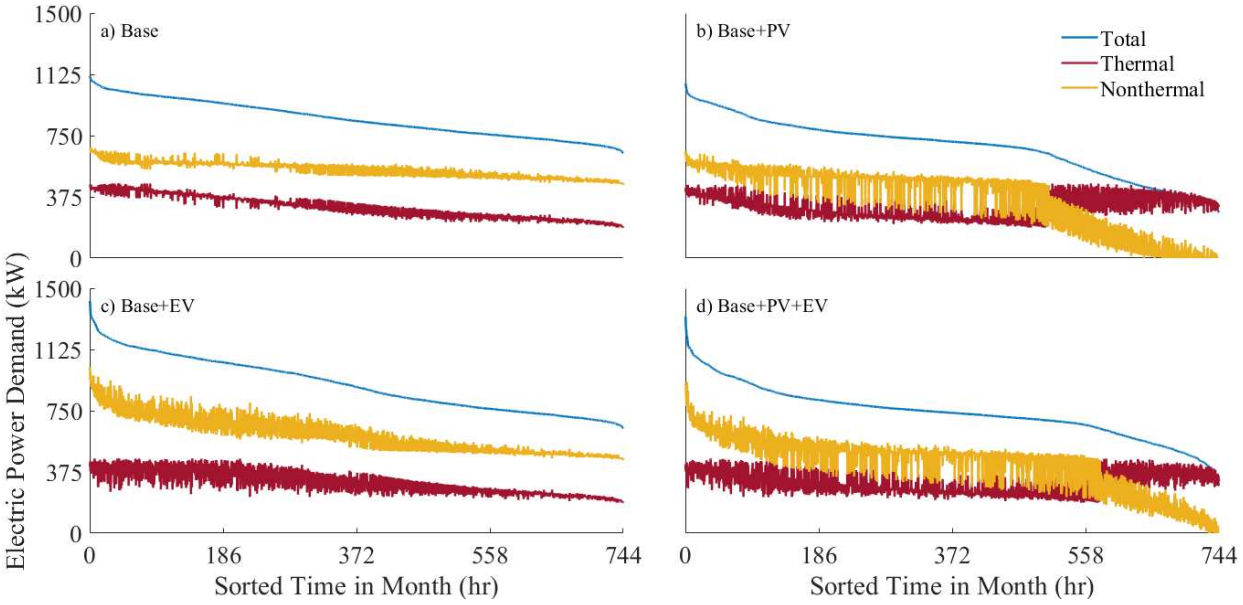

Figure 5.3: July load duration curves showing curves for total electric (Total), concurrent thermal loads (Thermal), and concurrent nonthermal (Nonthermal) loads for: (a) baseline building, (b) building with PV, (c) building with EV, and (d) building with PV and EV

5.2. Impact of building load profile on required energy and power of hybrid storage systems

The required energy sizes of thermal and battery energy storage for a given target level of peak demand reduction depend strongly on the load duration curves. Sizing is also sensitive to the maximum discharge power required by the battery, as batteries are not well suited for high discharge power. Increasing the discharge power of a battery at a fixed energy capacity can dramatically increase the capital expense [125]. Meanwhile, TES systems are, in this context, less

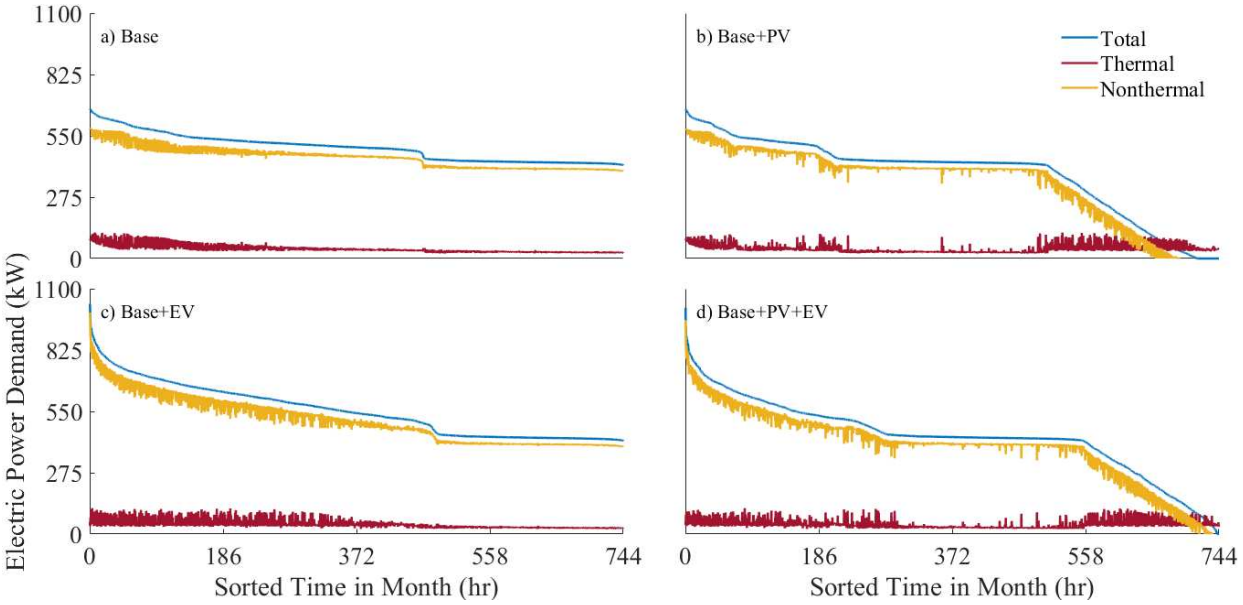

Figure 5.4: January load duration curves showing curves for total electric (Total), concurrent thermal loads (Thermal), and concurrent nonthermal (Nonthermal) loads for: (a) baseline building, (b) building with PV, (c) building with EV, and (d) building with PV and EV

sensitive to the discharge power, since shutting off cooling equipment can fully eliminate thermal electric loads. In fact, an active TES may also indirectly benefit from the advantage of passively storing thermal energy in the building structural materials, as it mitigates the need for high discharge powers for TES.

Figures 5.5 and 5.6 (Pages 57 and 60, respectively) show how the minimum required energy and power capacities for BES and TES change depending on the desired peak reduction, for both July and January, including (a) the required storage discharge capacity (kWh_e), (b) discharge power (kW), and (c) required C-rate. The thermal storage is sized to handle as much of the load as possible, with batteries added as soon as thermal storage cannot reduce the peak demand further. The required storage size increases with the desired peak reduction, but this differs depending on the scenario. For example, in July, a 200-kW peak reduction will require 1,000 kWh for the Base building, 400 kWh for Building+PV, 100 kWh for Building+EV, and 75 kWh for Building+EV+PV. In all scenarios, this 200-kW peak reduction could come from a battery, thermal

storage, or a hybrid system of the specified total system size. For comparison, in January, a 200-kW peak reduction cannot be achieved for the Base building, and requires 900 kWh in Building+PV, 200 kWh in Building+EV and 200 kWh in Building+EV+PV. In these scenarios, some of the storage must be from a battery because the thermal storage cannot deliver this level of peak reduction by itself. This shows one of the values of hybrid systems—TES is limited to cooling and heating loads, but when coordinated with batteries, the hybrid system can achieve greater peak demand reduction.

The results in Figure 5.5 provide other detailed insights into how these hybrid systems perform, discussed below for each building scenario:

Baseline Building (July): For the baseline building scenario (Figure 5.5(a)), a battery is not needed for any of the possible peak demand reduction levels. For the maximum peak reduction of 205 kW, the thermal storage would be 1,050 kWh with a power of 205 kW, which is a C-rate of about C/5. Lowering the peak reduction increases the C-rate, as this requires reducing the peak during fewer and fewer timesteps. In the extreme, the maximum C-rate is 4C, corresponding to a storage that reduces the peak during only one timestep in the entire month. This is unlikely to be cost effective, since there are fixed costs associated with any energy storage system (explored more in the next section). Therefore, it is more useful to look at higher levels of peak reduction of around 75 kW or more, which requires a maximum C-rate of 1C or less. There are diminishing returns from going to much larger sizes when the demand charge is the dominant component in the utility bill, as each additional kWh of storage shaves less and less peak demand. This is shown in the first plot, where the slope is at first shallow, and then increases rapidly above 75-100 kWh.

Building+PV (July): The load profile when including PV (Figure 5.5(b)) can still be flattened using only TES, but there are two key changes. Adding PV shortens the duration (but not

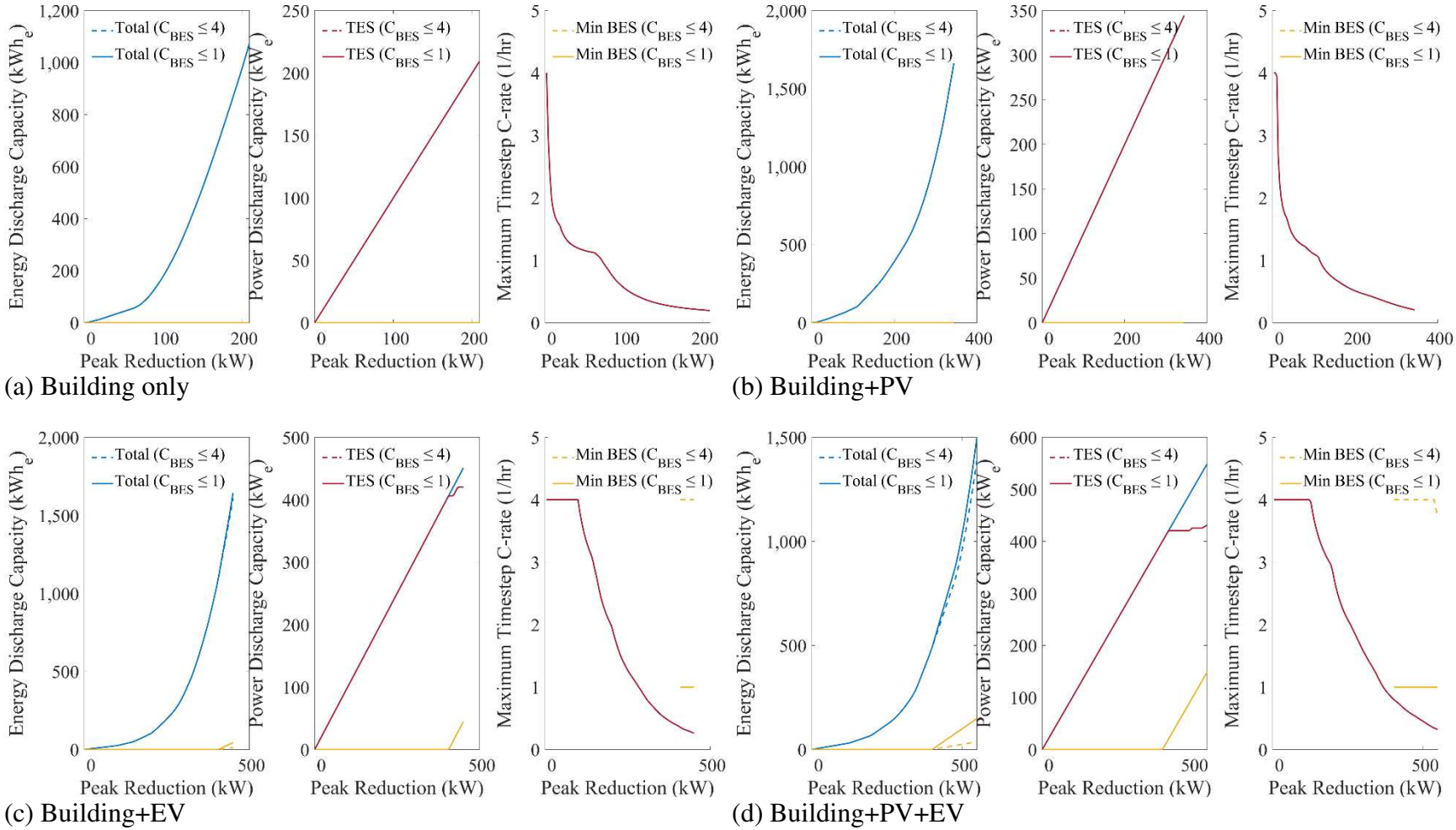

Figure 5.5: Impact of peak reduction on required hybrid energy storage capacity (including minimum battery size needed to meet nonthermal loads), required power for both hybrid components, and C-rate for both hybrid components for the four analyzed scenarios: (a) Baseline, (b) Building with PV, (c) Building with EV, and (d) Building with EV and PV; Summer design month

the magnitude) of the peak, which means it takes less energy storage for each kW of peak reduction. This is seen in the energy plots in Figure 5.5(a) and (b) where less storage is required for 100 kW of peak reduction (91 kWh) compared to the baseline building only scenario (178 kWh). This is also evident from the load duration curve (Figure 5.3), which has a sharper peak at the beginning of the curve. The maximum C-rate is also higher for these cases up to 100-kW peak reduction because less capacity is used for each kW of load reduction.

Adding PV also reduces the load in the middle of the day, providing more time to charge the storage and a lower 'flattened' peak that corresponds to the end of the curves in Figure 5.5. Again, the load duration curve shows this possibility by the steep drop off at the end of the curve ("tail")—a steeper load duration curve signifies more potential for peak reduction compared to a flat load duration curve. The efficiency of the thermal storage charging in the middle of the day will likely decrease because it is hotter outside (higher required temperature lift), but this effect is not included here.

Building+EV (July): The load profile for the Building+EV scenario (Figure 5.5(c)) shows larger peak-demand reduction potential than the Building+PV scenario because the load duration curve is steeper for the first 75% of the curve, and the absolute peak (1050 kW) is much higher than the Building or Building+PV scenarios (~700 kW). Although the peak reduction is larger, the resulting load for the maximum peak reduction (flat load duration curve) is still higher than for the baseline building or Building+PV scenarios.

The C-rate curve is also substantially higher for the Building+EV scenario, but it still ends around C/5 for the maximum peak reduction case. This means the storage strategy for the scenarios with EVs could either be a modest capacity with high power, or a modest power with a large energy capacity. For example, it could be a 150-kW / 50-kWh storage (3C) for a 150-kW peak reduction,

or a 400-kW / 1200-kWh storage (C/3) for a 400-kW peak reduction. For comparison, a 50-kWh storage for the building-only scenario would provide 50 kW of peak reduction (1C).

The introduction of extreme-fast EV chargers also requires battery storage past a 400-kW demand reduction. This 400 kW is the electric demand from air conditioning that corresponds to the peak in the load duration curve. The battery size then increases to shave each additional kW past 400-kW peak reduction. But the size differs depending on whether it is constrained to a 1C or 4C discharge rate. These are shown with the solid and dashed yellow lines, respectively, in Figure 5.5(c).

Building+PV+EV (July): Adding PV to the Building+EV scenario expands the possible peak-load reduction by allowing more charging during the low 'tail' of electric demand in the load duration curve. Like the Building+EV scenario, a battery is required past 400-kW peak demand reduction as TES already meets the thermal loads.

Figure 5.6 is laid out the same as Figure 5.5 but shows the results for January. Overall, all winter scenarios require some battery capacity since the cooling load is low in January (in many locations in the US there would be no cooling load). Results for January would be considerably different if considering a TES coupled with a heat-pump or electric-resistance heater for space heating in a colder climate, where utilization would be higher in winter months and lower in summer months.

Building only (January): A battery is required to reduce the peak by more than 90 kW, but adding a battery also enables more thermal storage. The battery provides access to more thermal load as we move further to the right on the load duration curve. For a given size of thermal storage, the C-rates will generally be lower in January than July because the load is much smaller. Above

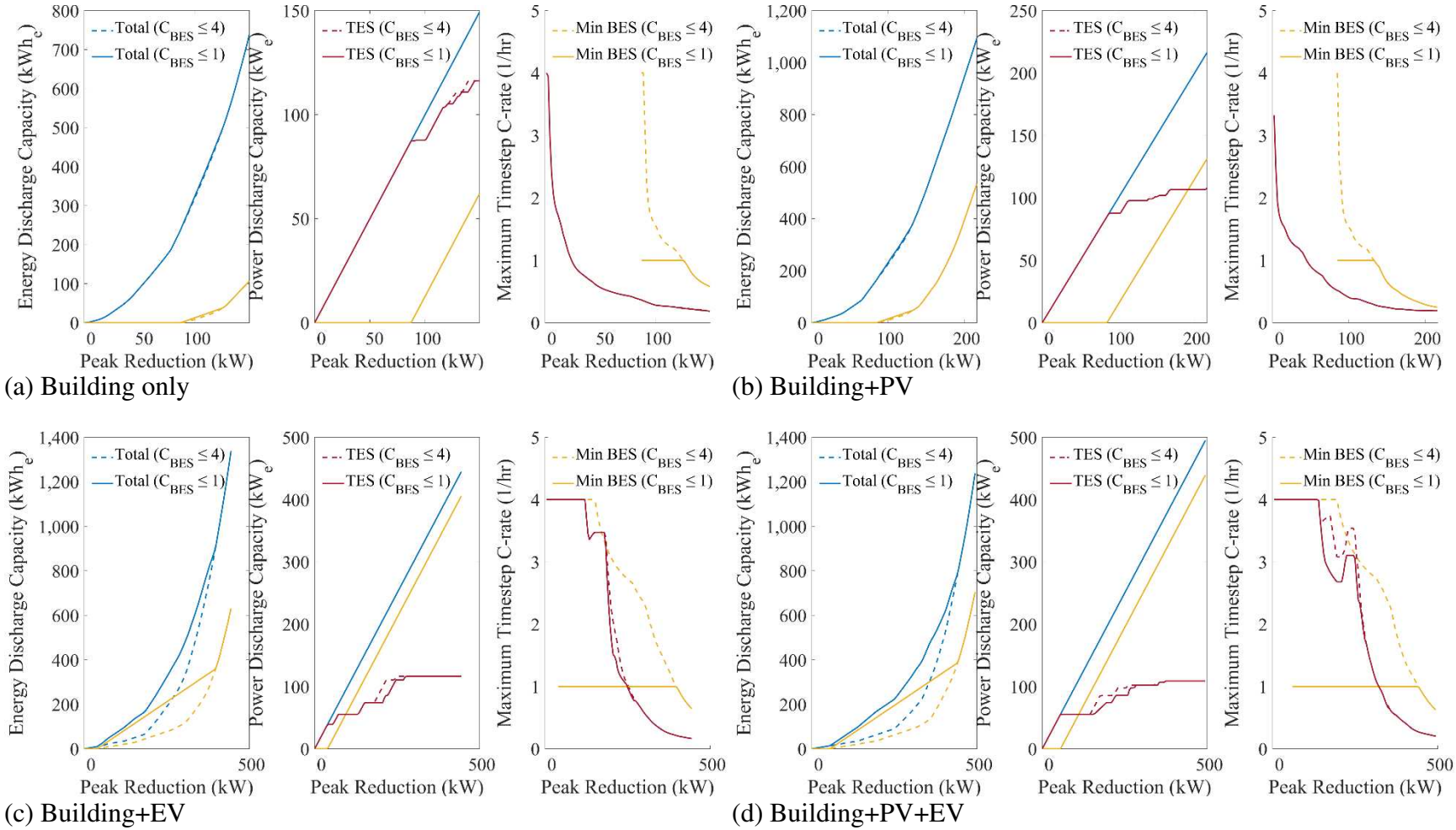

Figure 5.6: Impact of peak reduction on required hybrid energy storage capacity (including minimum battery size needed to meet nonthermal loads), required power for both hybrid components, and C-rate for both hybrid components for the four analyzed scenarios: (a) Baseline, (b) Building with PV, (c) Building with EV, and (d) Building with EV and PV; Winter design month

the 90-kW peak reduction, the C-rate for the battery is high, but a battery was not needed in July because all of the demand reduction could be met by the thermal storage.

Building+PV (January): Like July, adding PV increases the possible peak reduction. The maximum peak reduced by thermal storage is now 100 kW instead of 115 kW for the building-only case, because the PV moved that timestep from the beginning of the load duration curve to the end.

Building+EV (January): Adding extreme fast chargers pushes the need for a battery to lower target peak reduction levels because some EV charging is non-coincident with the thermal load. This is also true in July, but the ratio of the thermal electric load to the EV load makes this much less common. When adding the battery, the required C-rates are also large because of the short duration and high power of the EV charging events. The maximum peak demand is also much higher when adding EVs (425 kW), which means there is a need for a much larger battery.

Building+EV+PV (January): Adding PV does not substantially change the shape of these curves compared to the Building+EV scenario, but again increases the possible peak demand reduction (500 kW). For this and the Building+EV scenario, the battery must be upsized to avoid a power above 1C.

Figures 5.7 and 5.8 (Page 63) show hourly data for July for the baseline Building and Building+EV+PV scenarios respectively. The blue curve is the building without energy storage (Total), while the purple curve is the electric load due to air conditioning (Thermal). The sizing algorithm first determines how to discharge and charge the thermal storage to reduce the peak as much as possible. When the green dashed line (Thermal with TES) is above the Thermal base line, the thermal storage is being charged, and when it is below the Thermal base line, the thermal storage is being discharged. This drops the total electric load profile to the red line (Total with

TES). This red curve is showing the contribution of TES in a hybrid system and is not necessarily the curve that would result for a TES-only system. In the baseline building scenario, the thermal storage is charged at night and discharged during the day. This is typical of current installations of chiller-integrated thermal storge systems, including chilled-water tanks and ice storage systems.

Figure 5.8 has four graphs each showing (a) the maximum electrical energy displaced by thermal storage, (b) the maximum electrical energy displaced by battery storage, (c) the maximum discharge power required by TES, and (d) the maximum discharge power required by the battery. In these cases, the day that dictates the size for power and energy is different, and the right two figures are added because this scenario requires a battery for this level of demand reduction.

As the peak reduction is increased for the Building+EV+PV scenario, the green dashed line eventually hits zero (at hour 19), and there is no more thermal load to displace at that timestep. This is caused by the spikes due to EV charging. At these points, thermal storage is unable to independently reduce the peak, and a small battery is required to shave the total load to the desired level. The final load profile is the yellow dashed line, which is the total electric load at the meter when using thermal and battery storage (Total with TES+BES). The difference between the red and dashed/dotted yellow lines is the battery discharge power at that timestep.

In Figure 5.8(b), the load is flattened (i.e., all peaks shaved, and all valleys filled), meaning the flattened value on July 22 corresponds to the minimum possible peak for this month. Therefore, the storage dispatch strategy must follow the profile shown to obtain the maximum theoretical peak shaving. Although the peak BES energy utilization occurs on day 22 (Figure 5.8(b)), the peak power occurs on day 31 (Figure 5.8(d)), when the EV charging power is higher but for a shorter duration. Therefore, the C-rate limited power requirement is driven by the 31st day even though the 22nd day, with its two lower-power spikes, use more energy.

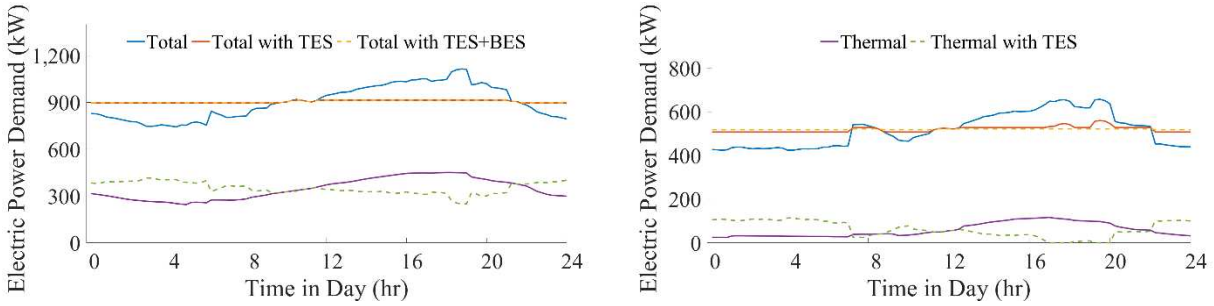

Figure 5.7: (a) Daily electric demand power profiles resulting from 200kW shaving in July for the Building scenario; (b) Daily electric demand power profiles resulting from 149-kW shaving in January for the Building scenario.

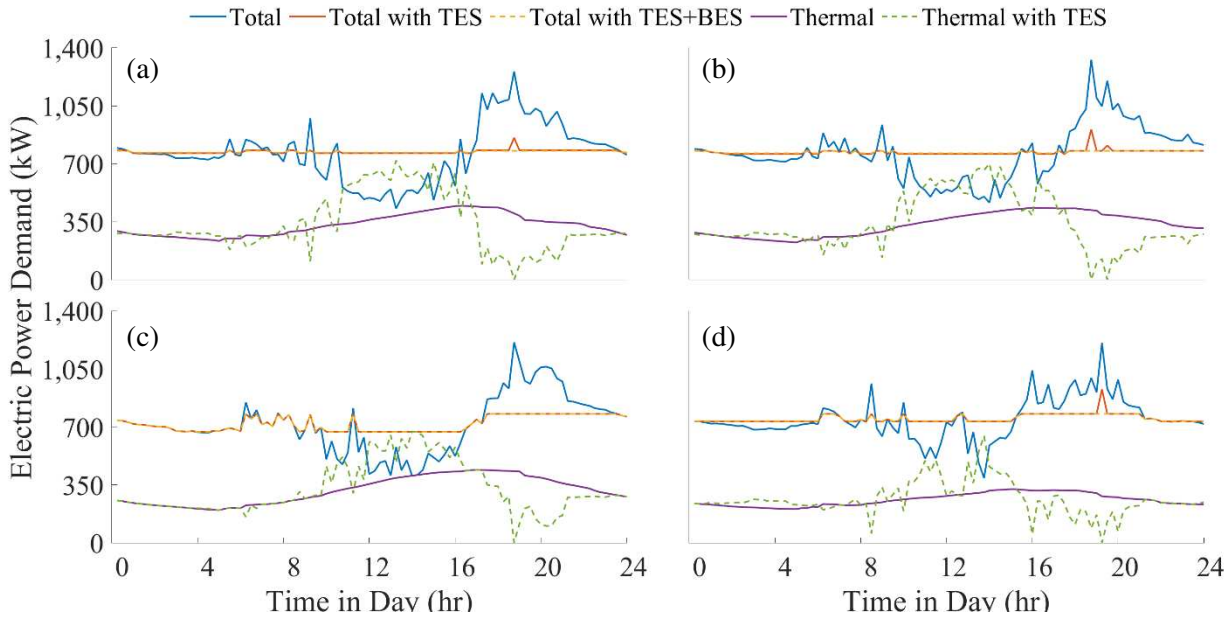

Figure 5.8: Daily electric demand power profiles resulting from maximum shaving (549 kW) in July for the Building+PV+EV scenario; (a) July 25 showing day with highest TES energy, (b) July 22 showing day with highest BES energy, (c) July 14 showing day with highest TES power, and (d) July 31 showing day with highest BES power

5.3. Annual performance and annualized cost savings of a hybrid storage system

One key takeaway from the results shown in the previous section is that sizing a hybrid system should not be performed using a single design month. The breakdown of energy and power capacities required from each component were quite different depending on the season. Thus, the

following analysis considers the annual performance and cost savings associated with hybrid storage systems.

The results shown here focus on the two extreme scenarios (Building only and Building+PV+EV). Figures 5.9(a) and 5.10(a) show the annual reduction in utility costs for the baseline building scenario and how it is impacted by battery and TES capacities. In these figures, the x-axis shows variations in TES energy discharge capacity, and the y-axis represents the BES energy discharge capacity. The colormap shows the annual utility cost savings, UCS, in thousands of dollars per year. Figure 5.9 shows results when the demand charge is assessed every month of the year, while Figure 5.10 shows demand charges only in the summer months. Both graphs show quasi-parallel contour lines with negative slopes meaning that peak demand shaving potential for battery and TES are nearly the same—a certain electric energy discharge capacity achieves the same peak shaving, whether it is from battery only, TES only, or a combination of the two. This is due to the strong correlation of the peak demand with the thermal load, particularly in summer. When demand charges are assessed for the entire year (Figure 5.9), the linearity is lost when TES is near 550 kWh_e because it reaches its maximum potential for demand reduction.

Figures 5.9(b) and 5.10(b) use the same axes, but the colormap shows equivalent full cycles for the battery. The number of equivalent full cycles are highest for a battery-only system, and peak near 120 for the entire year or 60 if used only in the summer. When the TES is small (near the y-axis), the battery is the primary component and therefore cycling increases with capacity as it is doing more and more of the hybrid system's total load shaving.

Converting some of the battery storage to TES will lower the battery cycles—moving along the constant total system size lines, the battery cycles drop. For example, switching a 900

kWh_e battery for a hybrid 600 kWh_e TES and 300 kWh_e battery drops the cycles from 120 to 50 and 60 to 15 for Figures 5.9 and 5.10, respectively.

For a large TES, increasing the battery capacity will reduce its cycling. This behavior is because with high TES capacity, TES can provide most of the peak shaving, leaving the battery idle and reducing its number of cycles. However, a system with a large thermal and battery energy storage could use the battery for other services, such as frequency regulation, contingency, or resiliency for the building owner during grid outages.

Figure 5.11 (Page 69) shows annual results for the Building+PV+EV scenario. The top two plots, (a) and (b), show the annual utility cost savings and battery equivalent full cycles. Plots (c) and (d) show annual cost savings after accounting for the storage systems' capital costs. In plot (c) the TES cost is equal to the battery cost, while plot (d) shows the outcome when TES is six times less expensive than batteries (see Section 4.3.3 for more details). Finally, plots (e) and (f) show the maximum and average C-rate for the battery, respectively.

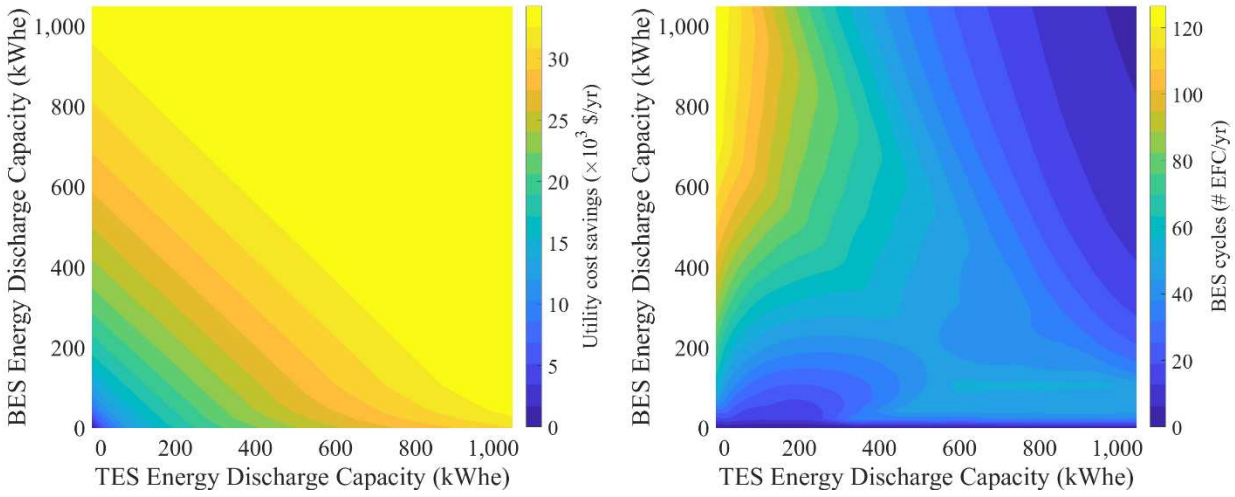

(a) (b)

Figure 5.9: Annual contour plots for (a) utility cost savings and (b) equivalent full cycles (EFC) for battery assuming TES discharge is prioritized, assuming **all months** have a demand charge for different energy capacities of TES (x-axis) and BES (y-axis) for the Building-only scenario

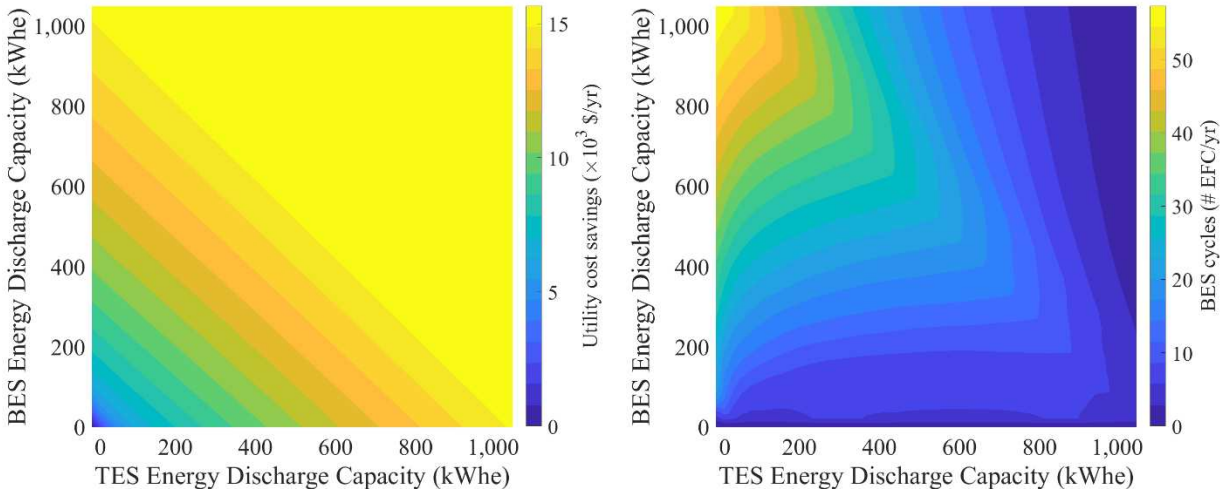

(a) (b)

Figure 5.10: Annual contour plots for (a) utility cost savings and (b) equivalent full cycles (EFC) for battery assuming TES discharge is prioritized, assuming **only summer months** have a demand charge for different energy capacities of TES (x-axis) and BES (y-axis) for the Building-only scenario

Figure 5.11(a) again shows the quasi-parallel curves, indicating the trend of reducing battery size and increasing TES size to achieve the same peak demand reduction, as reflected in utility costs savings. However, this quasi-parallel region is much smaller due to the relative size of the nonthermal load for this scenario, particularly in the winter.

For this scenario, consider different combinations of a 600 kWh_e hybrid system shown by the black lines. The utility cost savings potential is the same for the BES-only size of 600 kWh_e (indicated by circle) to a hybrid system of 300 kWh_e BES + 300 kWh_e TES (indicated by the star). Selecting a larger TES size and smaller battery size beyond this point will lead to lower battery cycling (Figure 5.11(b)) but will also lower the demand savings potential (Figure 5.11(a)). The system performance of a TES-only 600 kWh_e system (indicated by the square) achieves only about half of the total peak demand reduction-related savings.

For the case of equivalent capital costs shown in Figure 5.11(c), there is a maximum annualized cost savings where both energy storage devices provide equivalent load shaving

potential. This result is in part due to the assumption of a constant lifetime. If TES is less sensitive to cycling (as expected), than reducing the number of cycles experienced by the battery should increase its lifetime and decrease its annualized capital cost, making it more favorable to move along the black line to cases with lower battery cycling. This maximum region shifts to larger TES sizes when the TES is much less expensive than the battery (Figure 5.11(d)), but to achieve the maximum savings requires a battery size of at least 200 kWh_e because the thermal storage is limited in the amount of peak shaving it can do without a battery to address the nonthermal load. For the case of lower TES costs (Figure 5.11(d)), the range of TES sizes from 300 to 1,200 kWh_e all result in roughly the same annual cost savings once paired with a battery of about 300 kWh_e. On the smaller side of the range of TES capacities, the initial cost of purchasing the hybrid storge system will be the smallest. On the larger side, the initial investment cost will be much higher, but the TES will offer greater flexibility for future energy shifting, particularly as cooling loads increase and/or utilities implement higher demand or time-of-use electricity rates.

The bottom two plots show the battery C-rate maximum (Figure 5.11(e)) and average (Figure 5.11(f)). As the battery size is reduced, the C-rate increases. For a given TES system, small battery capacities lead to high C-rates. This keeps the desired battery capacity for the hybrid system away from the small capacities (< 300 kWh_e).

Taken as a whole, Figure 5.11 can be used to compare the three systems indicated by the circle (all battery), square (all TES), and star (hybrid system). A 600 kWh_e battery achieves 83% of the maximum possible peak reduction and would experience around 170 equivalent full cycles each year. It would also have a maximum C-rate of 0.85 and an average C-rate of 0.04. The hybrid system will achieve the same peak demand reduction but lowers the equivalent full cycles for the battery to 83. The maximum C-rate also increases to 1.0, but the average stays the same.

This shows that the hybrid system, even for a case where TES and batteries have the same capital cost, may be preferred because it lowers the battery equivalent full cycles by about 50%. This could extend the life of the battery and improve economics. More likely, the TES will have lower capital costs, making the economics even more favorable.

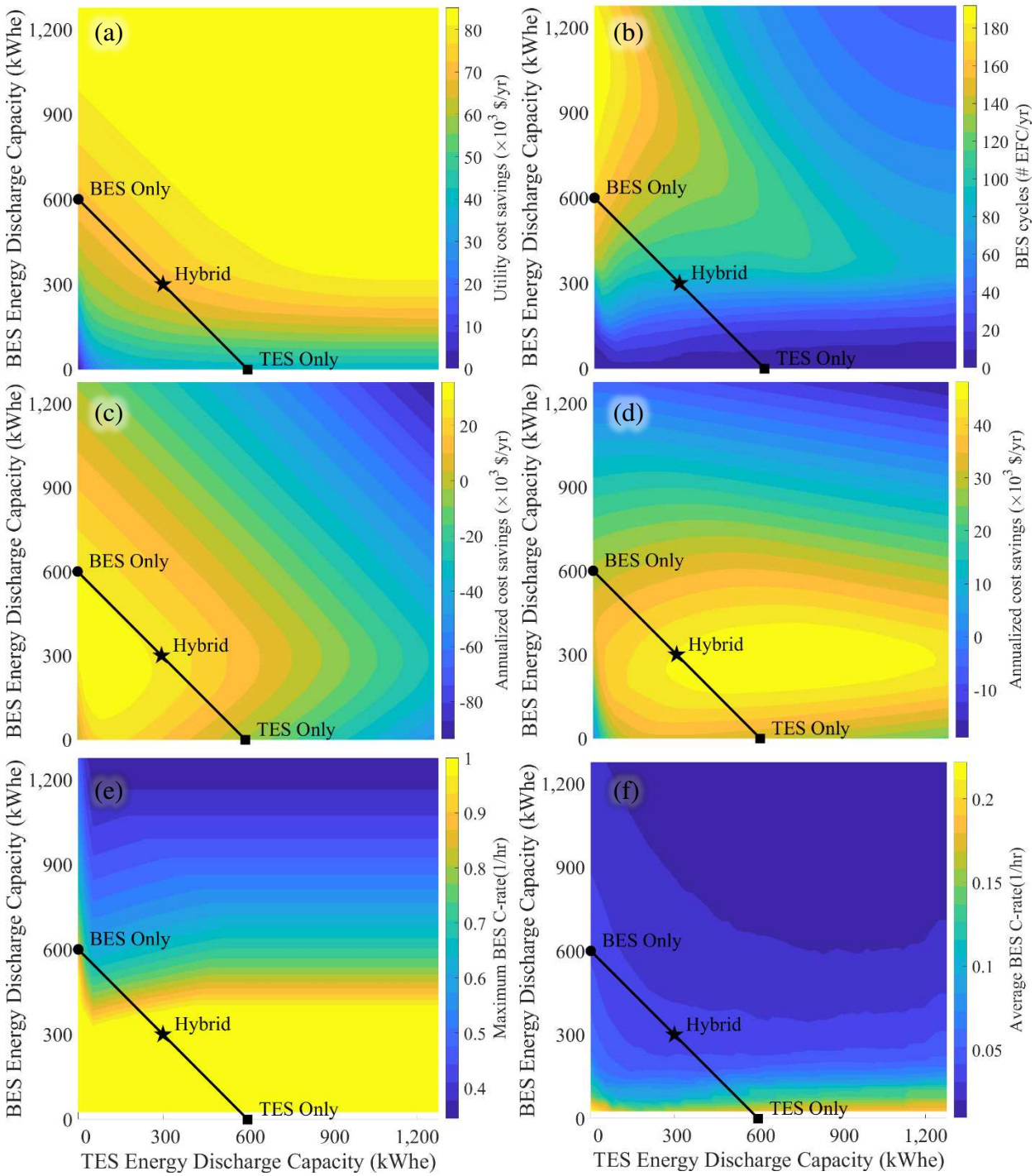

Figure 5.11: (a) Annual utility cost savings; (b) annual equivalent full cycles (EFC) for battery assuming TES discharge is prioritized; (c) annual total cost savings assuming TES capital expense is equal to BES; (d) annual total cost savings assuming TES capital expense is BES/6; (e) maximum C-rate experienced by battery for any timestep in year; (f) average C-rate experienced by battery for all discharging timesteps plotted for different energy capacities of TES (x-axis) and BES (y-axis) for Building+PV+EV scenario; the black line shows a constant storage capacity of 600 kWh_e

CHAPTER 6

CONCLUSIONS

This study proposes an analytical method for sizing a hybrid BES/TES system. The new method calculates the storage size necessary to obtain a target amount of peak reduction for design month or utility cost savings and annualized cost savings for a hybrid system of different sizes for an entire year.

This thesis uses a simulated big-box retail and grocery store in Phoenix, AZ with different combinations of EV charging and PV to evaluate the method and investigate potential tradeoffs and synergies of a hybrid battery/TES system. While the method is evaluated using cooling thermal loads, it can also be used for refrigeration, space heating, or water heating applications. This method shows how thermal storage can be used synergistically with a battery, and how these hybrid systems can be preferred to a standalone BES-only or TES-only system. Three key takeaways are:

1. Adding batteries to a TES system can increase the total system's load shaving potential (including increasing potential TES utilization) when the thermal load is small. This is particularly true when the building has onsite PV generation or EV charging, which add significant variability to the load shape. In particular, EV charging produce sudden and sharp nonthermal electric loads which require a battery.
2. Adding TES to a battery system can improve economics since TES often has a lower capital cost, and because it can significantly lower battery cycling, extending the battery life.
3. The optimal hybrid design is some combination of thermal and battery storage, and rarely only a battery-only or TES-only system.

There are several areas for potential improvement and future work. The method itself could be expanded to be more flexible with different utility rate structures. The current approach only allows specification of one demand charge with or without TOU rates; however, some utilities have implemented structures that utilize both all-time and on-peak type demand charges. Integrating physics-based models, rather than the simplified models presented in this study, for the energy storage systems would be an important step in making this approach more useful for actual sizing and dispatch recommendations to real building owners. A proper techno-economic analysis could account for many other variables, especially the relationship between cycling and device lifetime, which would improve understanding about the potential synergies for BES/TES hybrid systems. Additionally, future investigation could analyze different building types, EV charging scenarios, and investigate the impacts different EV, PV, TES, and BES performance and cost parameters. Finally, controls remain a challenge for hybrid systems. This approach (as with many optimization-based results) is agnostic to controls and simply specifies the best-case scenario that could happen if storage systems were dispatched in a particular way. Achieving the potential synergies described in this study depend on developing control strategies that are able to obtain peak demand reduction similar to what is predicted with an ideal dispatch.

REFERENCES CITED

[1] "How much energy is consumed in U.S. residential and commercial buildings?," *U.S. Energy Information Administration (EIA)*, May 2019 https://www.eia.gov/tools/faqs/faq.php?id=86&t=1 (accessed Jan. 17, 2020).

[2] M. Deru *et al.*, "U.S. Department of Energy Commercial Reference Building Models of the National Building Stock," National Renewable Energy Lab. (NREL), Golden, CO (United States), NREL/TP-5500-46861, Feb. 2011. doi: https://doi.org/10.2172/1009264.

[3] "Zero-Emission Vehicles." https://www.cpuc.ca.gov/zev/ (accessed Sep. 30, 2020).

[4] "Colorado EV Plan 2020 | Colorado Energy Office." https://energyoffice.colorado.gov/zero-emission-vehicles/colorado-ev-plan-2020 (accessed Sep. 30, 2020).

[5] H. Chen, T. N. Cong, W. Yang, C. Tan, Y. Li, and Y. Ding, "Progress in electrical energy storage system: A critical review," *Prog. Nat. Sci.*, vol. 19, no. 3, pp. 291–312, Mar. 2009, doi: 10.1016/j.pnsc.2008.07.014.

[6] L. Hu, Y. Liu, D. Wang, and J. Liu, "Battery Capacity Reduction for Stand-Alone PV Air Conditioner by Using Curtailed Electricity to Store Chilled Water as a Backup," in *Proceedings of the 11th International Symposium on Heating, Ventilation and Air Conditioning (ISHVAC 2019)*, Singapore, 2020, pp. 609–617, doi: 10.1007/978-981-13-9528-4_62.

[7] G. Comodi, F. Carducci, J. Y. Sze, N. Balamurugan, and A. Romagnoli, "Storing energy for cooling demand management in tropical climates: A techno-economic comparison between different energy storage technologies," *Energy*, vol. 121, pp. 676–694, Feb. 2017, doi: 10.1016/j.energy.2017.01.038.

[8] C. Luerssen, O. Gandhi, T. Reindl, C. Sekhar, and K. W. D. Cheong, "Levelised Cost of Thermal Energy Storage and Battery Storage to Store Solar PV Energy for Cooling Purpose," presented at the International Solar Energy Society, Sep. 2018, doi: 10.13140/RG.2.2.11361.56166.

[9] M. Ebrahimi, "Storing electricity as thermal energy at community level for demand side management," *Energy*, vol. 193, p. 116755, Feb. 2020, doi: 10.1016/j.energy.2019.116755.

[10] H. Lund *et al.*, "Energy Storage and Smart Energy Systems," *Int. J. Sustain. Energy Plan. Manag.*, vol. 11, pp. 3–14, Oct. 2016, doi: 10.5278/ijsepm.2016.11.2.

[11] D. Wu, M. Kintner-Meyer, T. Yang, and P. Balducci, "Analytical sizing methods for behind-the-meter battery storage," *J. Energy Storage*, vol. 12, pp. 297–304, Aug. 2017, doi: 10.1016/j.est.2017.04.009.

[12] G. S. Georgiou, P. Christodoulides, and S. A. Kalogirou, “Real-time energy convex optimization, via electrical storage, in buildings – A review,” *Renew. Energy*, vol. 139, pp. 1355–1365, Aug. 2019, doi: 10.1016/j.renene.2019.03.003.

[13] R. Kamal, F. Moloney, C. Wickramaratne, A. Narasimhan, and D. Y. Goswami, “Strategic control and cost optimization of thermal energy storage in buildings using EnergyPlus,” *Appl. Energy*, vol. 246, pp. 77–90, Jul. 2019, doi: 10.1016/j.apenergy.2019.04.017.

[14] B. Arcuri, C. Spataru, and M. Barrett, “Evaluation of ice thermal energy storage (ITES) for commercial buildings in cities in Brazil,” *Sustain. Cities Soc.*, vol. 29, pp. 178–192, Feb. 2017, doi: 10.1016/j.scs.2016.12.011.

[15] A. Sani Hassan, L. Cipcigan, and N. Jenkins, “Optimal battery storage operation for PV systems with tariff incentives,” *Appl. Energy*, vol. 203, pp. 422–441, Oct. 2017, doi: 10.1016/j.apenergy.2017.06.043.

[16] S. A. Ghoreishi-Madiseh, A. F. Kuyuk, H. Kalantari, and A. P. Sasmito, “Ice versus battery storage; a case for integration of renewable energy in refrigeration systems of remote sites,” *Energy Procedia*, vol. 159, pp. 60–65, Feb. 2019, doi: 10.1016/j.egypro.2018.12.018.

[17] S. Halbe, B. Chowdhury, and A. Abbas, “Mitigating Rebound Effect of Demand Response using Battery Energy Storage and Electric Water Heaters,” in *2019 IEEE 16th International Conference on Smart Cities: Improving Quality of Life Using ICT IoT and AI (HONET-ICT)*, Oct. 2019, pp. 095–099, doi: 10.1109/HONET.2019.8908081.

[18] Y. Iwafune, J. Kanamori, and H. Sakakibara, “A comparison of the effects of energy management using heat pump water heaters and batteries in photovoltaic-installed houses,” *Energy Convers. Manag.*, vol. 148, pp. 146–160, Sep. 2017, doi: 10.1016/j.enconman.2017.05.060.

[19] X. Wang and M. Dennis, “Influencing factors on the energy saving performance of battery storage and phase change cold storage in a PV cooling system,” *Energy Build.*, vol. 107, pp. 84–92, Nov. 2015, doi: 10.1016/j.enbuild.2015.08.008.

[20] X. Wang and M. Dennis, “A comparison of battery and phase change coolth storage in a PV cooling system under different climates,” *Sustain. Cities Soc.*, vol. 36, pp. 92–98, Jan. 2018, doi: 10.1016/j.scs.2017.09.035.

[21] Y. Sun, S. Wang, F. Xiao, and D. Gao, “Peak load shifting control using different cold thermal energy storage facilities in commercial buildings: A review,” *Energy Convers. Manag.*, vol. 71, pp. 101–114, Jul. 2013, doi: 10.1016/j.enconman.2013.03.026.

[22] G. P. Henze, C. Felsmann, and G. Knabe, “Evaluation of optimal control for active and passive building thermal storage,” *Int. J. Therm. Sci.*, vol. 43, no. 2, pp. 173–183, Feb. 2004, doi: 10.1016/j.ijthermalsci.2003.06.001.

[23] A. Hajiah and M. Krarti, “Optimal control of building storage systems using both ice storage and thermal mass – Part I: Simulation environment,” *Energy Convers. Manag.*, vol. 64, pp. 499–508, Dec. 2012, doi: 10.1016/j.enconman.2012.02.016.

[24] A. Hajiah and M. Krarti, “Optimal controls of building storage systems using both ice storage and thermal mass – Part II: Parametric analysis,” *Energy Convers. Manag.*, vol. 64, pp. 509–515, Dec. 2012, doi: 10.1016/j.enconman.2012.02.020.

[25] Y. Zhou, S. Cao, J. L. M. Hensen, and P. D. Lund, “Energy integration and interaction between buildings and vehicles: A state-of-the-art review,” *Renew. Sustain. Energy Rev.*, vol. 114, p. 109337, Oct. 2019, doi: 10.1016/j.rser.2019.109337.

[26] H. Akbari *et al.*, “Efficient energy storage technologies for photovoltaic systems,” *Sol. Energy*, vol. 192, pp. 144–168, Nov. 2019, doi: 10.1016/j.solener.2018.03.052.

[27] Y. Chen, P. Xu, J. Gu, F. Schmidt, and W. Li, “Measures to improve energy demand flexibility in buildings for demand response (DR): A review,” *Energy Build.*, vol. 177, pp. 125–139, Oct. 2018, doi: 10.1016/j.enbuild.2018.08.003.

[28] S. Al-Hallaj, G. Wilk, G. Crabtree, and M. Eberhard, “Overview of distributed energy storage for demand charge reduction,” *MRS Energy Sustain.*, vol. 5, ed 2018, doi: 10.1557/mre.2017.18.

[29] J. Neubauer and M. Simpson, “Deployment of Behind-The-Meter Energy Storage for Demand Charge Reduction,” National Renewable Energy Lab. (NREL), Golden, CO (United States), Golden, CO, Jan. 2015.

[30] D. Wu, M. Kintner-Meyer, Tao Yang, and P. Balducci, “Economic analysis and optimal sizing for behind-the-meter battery storage,” in *2016 IEEE Power and Energy Society General Meeting (PESGM)*, Jul. 2016, pp. 1–5, doi: 10.1109/PESGM.2016.7741210.

[31] D. Wu, M. Kintner-Meyer, T. Yang, and P. Balducci, “Analytical sizing methods for behind-the-meter battery storage,” *J. Energy Storage*, vol. 12, pp. 297–304, Aug. 2017, doi: 10.1016/j.est.2017.04.009.

[32] J. Mostert and B. Bekker, “Estimating financial viability of behind-the-meter peak shaving based on load profile shape: a shopping mall case study,” in *2020 International SAUPEC/RobMech/PRASA Conference*, Jan. 2020, pp. 1–6, doi: 10.1109/SAUPEC/RobMech/PRASA48453.2020.9041083.

[33] A. Zurfi, G. Albayati, and J. Zhang, “Economic feasibility of residential behind-the-meter battery energy storage under energy time-of-use and demand charge rates,” in *2017 IEEE 6th International Conference on Renewable Energy Research and Applications (ICRERA)*, Nov. 2017, pp. 842–849, doi: 10.1109/ICRERA.2017.8191179.

[34] Y. Chen, V. Chandna, Y. Huang, M. J. E. Alam, O. Ahmed, and L. Smith, “Coordination of Behind-the-Meter Energy Storage and Building Loads: Optimization with Deep Learning Model,” in *Proceedings of the Tenth ACM International Conference on Future*

Energy Systems, Phoenix, AZ, USA, Jun. 2019, pp. 492–499, doi: 10.1145/3307772.3331025.

[35] M. Kharseh and Prof. H. Wallbaum, "The effect of different working parameters on the optimal size of a battery for grid-connected PV systems," *Energy Procedia*, vol. 122, pp. 595–600, Sep. 2017, doi: 10.1016/j.egypro.2017.07.355.

[36] L. Zhou, Y. Zhang, X. Lin, C. Li, Z. Cai, and P. Yang, "Optimal Sizing of PV and BESS for a Smart Household Considering Different Price Mechanisms," *IEEE Access*, vol. 6, pp. 41050–41059, 2018, doi: 10.1109/ACCESS.2018.2845900.

[37] K. Heine, A. Thatte, and P. C. Tabares-Velasco, "A simulation approach to sizing batteries for integration with net-zero energy residential buildings," *Renew. Energy*, vol. 139, pp. 176–185, Aug. 2019, doi: 10.1016/j.renene.2019.02.033.

[38] K. Faraj, M. Khaled, J. Faraj, F. Hachem, and C. Castelain, "Phase change material thermal energy storage systems for cooling applications in buildings: A review," *Renew. Sustain. Energy Rev.*, vol. 119, p. 109579, Mar. 2020, doi: 10.1016/j.rser.2019.109579.

[39] S. Rashidi, H. Shamsabadi, J. A. Esfahani, and S. Harmand, "A review on potentials of coupling PCM storage modules to heat pipes and heat pumps," *J. Therm. Anal. Calorim.*, Nov. 2019, doi: 10.1007/s10973-019-08930-1.

[40] E. Guelpa and V. Verda, "Thermal energy storage in district heating and cooling systems: A review," *Appl. Energy*, vol. 252, p. 113474, Oct. 2019, doi: 10.1016/j.apenergy.2019.113474.

[41] I. Sarbu and C. Sebarchievici, "A Comprehensive Review of Thermal Energy Storage," *Sustainability*, vol. 10, no. 1, p. 191, Jan. 2018, doi: 10.3390/su10010191.

[42] S. Kahwaji, M. B. Johnson, A. C. Kheirabadi, D. Groulx, and M. A. White, "A comprehensive study of properties of paraffin phase change materials for solar thermal energy storage and thermal management applications," *Energy*, vol. 162, pp. 1169–1182, Nov. 2018, doi: 10.1016/j.energy.2018.08.068.

[43] X. Wang, H. Chen, Y. Xu, L. Wang, and S. HU, "Advances and prospects in thermal energy storage: A critical review," *Chin. Sci. Bull.*, vol. 62, pp. 1602–1610, May 2017, doi: 10.1360/N972016-00663.

[44] A. Arteconi, N. J. Hewitt, and F. Polonara, "State of the art of thermal storage for demand-side management," *Appl. Energy*, vol. 93, pp. 371–389, May 2012, doi: 10.1016/j.apenergy.2011.12.045.

[45] N. A. Aziz, N. A. M. Amin, M. S. A. Majid, and I. Zaman, "Thermal energy storage (TES) technology for active and passive cooling in buildings: A Review," *MATEC Web Conf.*, vol. 225, p. 03022, 2018, doi: 10.1051/matecconf/201822503022.

[46] Y. Sun, S. Wang, F. Xiao, and D. Gao, "Peak load shifting control using different cold thermal energy storage facilities in commercial buildings: A review," *Energy Convers. Manag.*, vol. 71, pp. 101–114, Jul. 2013, doi: 10.1016/j.enconman.2013.03.026.

[47] J. E. Braun, "Reducing energy costs and peak electrical demand through optimal control of building thermal storage," 1990.

[48] K. R. Keeney and J. E. Braun, "Application of building precooling to reduce peak cooling requirements," Art. no. CONF-9702141-, Dec. 1997, Accessed: Jul. 30, 2020. [Online]. Available: https://www.osti.gov/biblio/345252-application-building-precooling-reduce-peak-cooling-requirements.

[49] P. Xu, P. Haves, M. A. Piette, and J. Braun, "Peak demand reduction from pre-cooling with zone temperature reset in an office building," Aug. 2004, Accessed: Jul. 30, 2020. [Online]. Available: https://escholarship.org/uc/item/1205612d#author.

[50] K. Lee and J. E. Braun, "An experimental evaluation of demand limiting using building thermal mass in a small commercial building," *ASHRAE Trans.*, vol. 112, pp. 559–571, Jan. 2006.

[51] S. Wijesuriya, M. Brandt, and P. C. Tabares-Velasco, "Parametric analysis of a residential building with phase change material (PCM)-enhanced drywall, precooling, and variable electric rates in a hot and dry climate," *Appl. Energy*, vol. 222, pp. 497–514, Jul. 2018, doi: 10.1016/j.apenergy.2018.03.119.

[52] P. C. Tabares-Velasco, A. Speake, M. Harris, A. Newman, T. Vincent, and M. Lanahan, "A modeling framework for optimization-based control of a residential building thermostat for time-of-use pricing," *Appl. Energy*, vol. 242, pp. 1346–1357, May 2019, doi: 10.1016/j.apenergy.2019.01.241.

[53] J. Deason, M. Wei, G. Leventis, S. Smith, and L. Schwartz, "Electrification of buildings and industry in the United States: Drivers, barriers, prospects, and policy approaches," Energy Analysis and Environmental Impacts Division Lawrence Berkeley National Laboratory, LBNL-2001133, 2018.

[54] T. T. Mai *et al.*, "Electrification Futures Study: Scenarios of Electric Technology Adoption and Power Consumption for the United States," NREL/TP--6A20-71500, 1459351, Jun. 2018. doi: 10.2172/1459351.

[55] I. Sarbu and C. Sebarchievici, "General review of ground-source heat pump systems for heating and cooling of buildings," *Energy Build.*, vol. 70, pp. 441–454, Feb. 2014, doi: 10.1016/j.enbuild.2013.11.068.

[56] Á. Á. Pardiñas, M. J. Alonso, R. Diz, K. H. Kvalsvik, and J. Fernández-Seara, "State-of-the-art for the use of phase-change materials in tanks coupled with heat pumps," *Energy Build.*, vol. 140, pp. 28–41, Apr. 2017, doi: 10.1016/j.enbuild.2017.01.061.

[57] S. Maaraoui, D. Clodic, and P. Dalicieux, “Heat Pump With a Condenser Including Solid-Liquid Phase Change Material,” *Int. Refrig. Air Cond. Conf.*, Jan. 2012, [Online]. Available: https://docs.lib.purdue.edu/iracc/1194.

[58] A. Arteconi and F. Polonara, “Assessing the Demand Side Management Potential and the Energy Flexibility of Heat Pumps in Buildings,” *Energies*, vol. 11, no. 7, p. 1846, Jul. 2018, doi: 10.3390/en11071846.

[59] N. J. Kelly, P. G. Tuohy, and A. D. Hawkes, “Performance assessment of tariff-based air source heat pump load shifting in a UK detached dwelling featuring phase change-enhanced buffering,” *Appl. Therm. Eng.*, vol. 71, no. 2, pp. 809–820, Oct. 2014, doi: 10.1016/j.applthermaleng.2013.12.019.

[60] D. Zou *et al.*, “Experimental research of an air-source heat pump water heater using water-PCM for heat storage,” *Appl. Energy*, vol. 206, pp. 784–792, Nov. 2017, doi: 10.1016/j.apenergy.2017.08.209.

[61] H. M. Teamah and M. F. Lightstone, “Numerical study of the electrical load shift capability of a ground source heat pump system with phase change thermal storage,” *Energy Build.*, vol. 199, pp. 235–246, Sep. 2019, doi: 10.1016/j.enbuild.2019.06.056.

[62] M. Pau, F. Cunsolo, J. Vivian, F. Ponci, and A. Monti, “Optimal Scheduling of Electric Heat Pumps Combined with Thermal Storage for Power Peak Shaving,” in *2018 IEEE International Conference on Environment and Electrical Engineering and 2018 IEEE Industrial and Commercial Power Systems Europe (EEEIC / I CPS Europe)*, Jun. 2018, pp. 1–6, doi: 10.1109/EEEIC.2018.8494592.

[63] F. Agyenim and N. Hewitt, “The development of a finned phase change material (PCM) storage system to take advantage of off-peak electricity tariff for improvement in cost of heat pump operation,” *Energy Build.*, vol. 42, no. 9, pp. 1552–1560, Sep. 2010, doi: 10.1016/j.enbuild.2010.03.027.

[64] L. Cabrol and P. Rowley, “Towards low carbon homes – A simulation analysis of building-integrated air-source heat pump systems,” *Energy Build.*, vol. 48, pp. 127–136, May 2012, doi: 10.1016/j.enbuild.2012.01.019.

[65] M. Akmal and B. Fox, “Modelling and Simulation of Underfloor Heating System Supplied from Heat Pump,” in *2016 UKSim-AMSS 18th International Conference on Computer Modelling and Simulation (UKSim)*, Apr. 2016, pp. 246–251, doi: 10.1109/UKSim.2016.13.

[66] A. Arteconi, N. J. Hewitt, and F. Polonara, “Domestic demand-side management (DSM): Role of heat pumps and thermal energy storage (TES) systems,” *Appl. Therm. Eng.*, vol. 51, no. 1, pp. 155–165, Mar. 2013, doi: 10.1016/j.applthermaleng.2012.09.023.

[67] B. Baeten, F. Rogiers, and L. Helsen, “Reduction of heat pump induced peak electricity use and required generation capacity through thermal energy storage and demand

response," *Appl. Energy*, vol. 195, pp. 184–195, Jun. 2017, doi: 10.1016/j.apenergy.2017.03.055.

[68] J. Chen and J. Yu, "Dynamic simulation of an air-source heat pump water heater using novel modified evaporator model," *Appl. Therm. Eng.*, vol. 144, pp. 469–478, Nov. 2018, doi: 10.1016/j.applthermaleng.2018.08.085.

[69] F. D'Ettorre, M. De Rosa, P. Conti, D. Testi, and D. Finn, "Mapping the energy flexibility potential of single buildings equipped with optimally-controlled heat pump, gas boilers and thermal storage," *Sustain. Cities Soc.*, vol. 50, p. 101689, Oct. 2019, doi: 10.1016/j.scs.2019.101689.

[70] J. Fadejev and J. Kurnitski, "Geothermal energy piles and boreholes design with heat pump in a whole building simulation software," *Energy Build.*, vol. 106, pp. 23–34, Nov. 2015, doi: 10.1016/j.enbuild.2015.06.014.

[71] H. Moon, H. Kim, and Y. Nam, "Study on the Optimum Design of a Ground Heat Pump System Using Optimization Algorithms," *Energies*, vol. 12, no. 21, p. 4033, Jan. 2019, doi: 10.3390/en12214033.

[72] R. Hirmiz, H. M. Teamah, M. F. Lightstone, and J. S. Cotton, "Performance of heat pump integrated phase change material thermal storage for electric load shifting in building demand side management," *Energy Build.*, vol. 190, pp. 103–118, May 2019, doi: 10.1016/j.enbuild.2019.02.026.

[73] K. Bakirci and B. Yuksel, "Experimental thermal performance of a solar source heat-pump system for residential heating in cold climate region," *Appl. Therm. Eng.*, vol. 31, no. 8, pp. 1508–1518, Jun. 2011, doi: 10.1016/j.applthermaleng.2011.01.039.

[74] O. Comakli, K. Kaygusuz, and T. Ayhan, "Solar-assisted heat pump and energy storage for residential heating," *Sol. Energy*, vol. 51, no. 5, pp. 357–366, Jan. 1993, doi: 10.1016/0038-092X(93)90148-H.

[75] H. Huang, Y. Xiao, J. Lin, T. Zhou, Y. Liu, and Q. Zhao, "Thermal characteristics of a seasonal solar assisted heat pump heating system with an underground tank," *Sustain. Cities Soc.*, vol. 53, p. 101910, Feb. 2020, doi: 10.1016/j.scs.2019.101910.

[76] M. Ali, J. Jokisalo, K. Siren, and M. Lehtonen, "Combining the Demand Response of direct electric space heating and partial thermal storage using LP optimization," *Electr. Power Syst. Res.*, vol. 106, pp. 160–167, Jan. 2014, doi: 10.1016/j.epsr.2013.08.017.

[77] X. Liu, P. Zhang, A. Pimm, D. Feng, and M. Zheng, "Optimal design and operation of PV-battery systems considering the interdependency of heat pumps," *J. Energy Storage*, vol. 23, pp. 526–536, Jun. 2019, doi: 10.1016/j.est.2019.04.026.

[78] J. Niu, Z. Tian, Y. Lu, and H. Zhao, "Flexible dispatch of a building energy system using building thermal storage and battery energy storage," *Appl. Energy*, vol. 243, pp. 274–287, Jun. 2019, doi: 10.1016/j.apenergy.2019.03.187.

[79] M. Leśko, W. Bujalski, and K. Futyma, “Operational optimization in district heating systems with the use of thermal energy storage,” *Energy*, vol. 165, pp. 902–915, Dec. 2018, doi: 10.1016/j.energy.2018.09.141.

[80] A. S. O. Ogunjuyigbe, T. R. Ayodele, and O. E. Oladimeji, “Management of loads in residential buildings installed with PV system under intermittent solar irradiation using mixed integer linear programming,” *Energy Build.*, vol. 130, pp. 253–271, Oct. 2016, doi: 10.1016/j.enbuild.2016.08.042.

[81] H. Mehrjerdi and E. Rakhshani, “Optimal operation of hybrid electrical and thermal energy storage systems under uncertain loading condition,” *Appl. Therm. Eng.*, vol. 160, p. 114094, Sep. 2019, doi: 10.1016/j.applthermaleng.2019.114094.

[82] Z. Zhou, P. Liu, Z. Li, and W. Ni, “An engineering approach to the optimal design of distributed energy systems in China,” *Appl. Therm. Eng.*, vol. 53, no. 2, pp. 387–396, May 2013, doi: 10.1016/j.applthermaleng.2012.01.067.

[83] K. M. Powell *et al.*, “Thermal energy storage to minimize cost and improve efficiency of a polygeneration district energy system in a real-time electricity market,” *Energy*, vol. 113, pp. 52–63, Oct. 2016, doi: 10.1016/j.energy.2016.07.009.

[84] A. Baniasadi, D. Habibi, W. Al-Saedi, M. A. S. Masoum, C. K. Das, and N. Mousavi, “Optimal sizing design and operation of electrical and thermal energy storage systems in smart buildings,” *J. Energy Storage*, vol. 28, p. 101186, Apr. 2020, doi: 10.1016/j.est.2019.101186.

[85] F. Ren, J. Wang, S. Zhu, and Y. Chen, “Multi-objective optimization of combined cooling, heating and power system integrated with solar and geothermal energies,” *Energy Convers. Manag.*, vol. 197, p. 111866, Oct. 2019, doi: 10.1016/j.enconman.2019.111866.

[86] H. Molavi and M. M. Ardehali, “Utility demand response operation considering day-of-use tariff and optimal operation of thermal energy storage system for an industrial building based on particle swarm optimization algorithm,” *Energy Build.*, vol. 127, pp. 920–929, Sep. 2016, doi: 10.1016/j.enbuild.2016.06.056.

[87] S. Ikeda and R. Ooka, “Metaheuristic optimization methods for a comprehensive operating schedule of battery, thermal energy storage, and heat source in a building energy system,” *Appl. Energy*, vol. 151, pp. 192–205, Aug. 2015, doi: 10.1016/j.apenergy.2015.04.029.

[88] R. Gelleschus, M. Böttiger, P. Stange, and T. Bocklisch, “Comparison of optimization solvers in the model predictive control of a PV-battery-heat pump system,” *Energy Procedia*, vol. 155, pp. 524–535, Nov. 2018, doi: 10.1016/j.egypro.2018.11.028.

[89] S. A. Mansouri, A. Ahmarinejad, M. Ansarian, M. S. Javadi, and J. P. S. Catalao, “Stochastic planning and operation of energy hubs considering demand response programs using Benders decomposition approach,” *Int. J. Electr. Power Energy Syst.*, vol. 120, p. 106030, Sep. 2020, doi: 10.1016/j.ijepes.2020.106030.

[90] S. Senemar, M. Rastegar, M. Dabbaghjamanesh, and N. D. Hatziargyriou, "Dynamic Structural Sizing of Residential Energy Hubs," *IEEE Trans. Sustain. Energy*, pp. 1–1, 2019, doi: 10.1109/TSTE.2019.2921110.

[91] S. Pazouki and M.-R. Haghifam, "Optimal planning and scheduling of energy hub in presence of wind, storage and demand response under uncertainty," *Int. J. Electr. Power Energy Syst.*, vol. 80, pp. 219–239, Sep. 2016, doi: 10.1016/j.ijepes.2016.01.044.

[92] A. Najafi *et al.*, "Uncertainty-Based Models for Optimal Management of Energy Hubs Considering Demand Response," *Energies*, vol. 12, no. 8, p. 1413, Jan. 2019, doi: 10.3390/en12081413.

[93] Y. Wang, N. Zhang, Z. Zhuo, C. Kang, and D. Kirschen, "Mixed-integer linear programming-based optimal configuration planning for energy hub: Starting from scratch," *Appl. Energy*, vol. 210, pp. 1141–1150, Jan. 2018, doi: 10.1016/j.apenergy.2017.08.114.

[94] M. Rastegar and M. Fotuhi-Firuzabad, "Load management in a residential energy hub with renewable distributed energy resources," *Energy Build.*, vol. 107, pp. 234–242, Nov. 2015, doi: 10.1016/j.enbuild.2015.07.028.

[95] X. Jin, K. Baker, D. Christensen, and S. Isley, "Foresee: A user-centric home energy management system for energy efficiency and demand response," *Appl. Energy*, vol. 205, pp. 1583–1595, Nov. 2017, doi: 10.1016/j.apenergy.2017.08.166.

[96] A. Ashouri, S. S. Fux, M. J. Benz, and L. Guzzella, "Optimal design and operation of building services using mixed-integer linear programming techniques," *Energy*, vol. 59, pp. 365–376, Sep. 2013, doi: 10.1016/j.energy.2013.06.053.

[97] M. Kintner-Meyer and A. F. Emery, "Optimal control of an HVAC system using cold storage and building thermal capacitance," *Energy Build.*, vol. 23, no. 1, pp. 19–31, Oct. 1995, doi: 10.1016/0378-7788(95)00917-M.

[98] C. Yan, W. Shi, X. Li, and Y. Zhao, "Optimal design and application of a compound cold storage system combining seasonal ice storage and chilled water storage," *Appl. Energy*, vol. 171, pp. 1–11, Jun. 2016, doi: 10.1016/j.apenergy.2016.03.005.

[99] X. Song, L. Liu, T. Zhu, S. Chen, and Z. Cao, "Study of economic feasibility of a compound cool thermal storage system combining chilled water storage and ice storage," *Appl. Therm. Eng.*, vol. 133, pp. 613–621, Mar. 2018, doi: 10.1016/j.applthermaleng.2018.01.063.

[100] D. Wang, L. Hu, Y. Liu, and J. Liu, "Performance of off-grid photovoltaic cooling system with two-stage energy storage combining battery and cold water tank," *Energy Procedia*, vol. 132, pp. 574–579, Oct. 2017, doi: 10.1016/j.egypro.2017.09.745.

[101] W. Hu, C. C. Chai, W. Yang, and R. Yu, "Comprehensive modeling and joint optimization of ice thermal and battery energy storage with provision of grid services," in *TENCON*

2017 - 2017 IEEE Region 10 Conference, Nov. 2017, pp. 528–533, doi: 10.1109/TENCON.2017.8227920.

[102] C. J. Meinrenken and A. Mehmani, "Concurrent optimization of thermal and electric storage in commercial buildings to reduce operating cost and demand peaks under time-of-use tariffs," *Appl. Energy*, vol. 254, p. 113630, Nov. 2019, doi: 10.1016/j.apenergy.2019.113630.

[103] F. Kung, S. Frank, J. Scheib, W. B. Heredia, and S. Pless, "Supervisory Control of Loads and Energy Storage in Next-Generation Zero Energy Buildings," *Renew. Energy*, p. 71, Sep. 2016.

[104] J. Borland, J. Moore, C. Poncho, T. Tanaka, and H. McClure, "> 94.5% Reduction in Grid-Buy Electricity and Elimination of AM PM Energy Peaks/Spikes by Optimizing Energy Usage and Integration of Customer Self-Supply Rooftop Solar PV with Electrical Thermal (Hot Cold) Storage Batteries: A Case Study for Residential Hawaii," in *2017 IEEE 44th Photovoltaic Specialist Conference (PVSC)*, Jun. 2017, pp. 2947–2951, doi: 10.1109/PVSC.2017.8366739.

[105] D. T. Vedullapalli, R. Hadidi, and B. Schroeder, "Combined HVAC and Battery Scheduling for Demand Response in a Building," *IEEE Trans. Ind. Appl.*, vol. 55, no. 6, pp. 7008–7014, Nov. 2019, doi: 10.1109/TIA.2019.2938481.

[106] A. A. Shukhobodskiy and G. Colantuono, "RED WoLF: Combining a battery and thermal energy reservoirs as a hybrid storage system," *Appl. Energy*, vol. 274, p. 115209, Sep. 2020, doi: 10.1016/j.apenergy.2020.115209.

[107] E. O'Shaughnessy, D. Cutler, K. Ardani, and R. Margolis, "Solar plus: Optimization of distributed solar PV through battery storage and dispatchable load in residential buildings," *Appl. Energy*, vol. 213, pp. 11–21, Mar. 2018, doi: 10.1016/j.apenergy.2017.12.118.

[108] H. Gong, V. Rallabandi, D. M. Ionel, Colliver, S. Duerr, and C. Ababei, "Net Zero Energy Houses with Dispatchable Solar PV Power Supported by Electric Water Heater and Battery Energy Storage," in *2018 IEEE Energy Conversion Congress and Exposition (ECCE)*, Sep. 2018, pp. 2498–2503, doi: 10.1109/ECCE.2018.8557720.

[109] C. J. C. Williams, J. O. Binder, and T. Kelm, "Demand side management through heat pumps, thermal storage and battery storage to increase local self-consumption and grid compatibility of PV systems," in *2012 3rd IEEE PES Innovative Smart Grid Technologies Europe (ISGT Europe)*, Oct. 2012, pp. 1–6, doi: 10.1109/ISGTEurope.2012.6465874.

[110] S. Zurmühlen *et al.*, "Potential and Optimal Sizing of Combined Heat and Electrical Storage in Private Households," *Energy Procedia*, vol. 99, pp. 174–181, Nov. 2016, doi: 10.1016/j.egypro.2016.10.108.

[111] D. Steen, M. Stadler, G. Cardoso, M. Groissböck, N. DeForest, and C. Marnay, "Modeling of thermal storage systems in MILP distributed energy resource models," *Appl. Energy*, vol. 137, pp. 782–792, Jan. 2015, doi: 10.1016/j.apenergy.2014.07.036.

[112] T. Wakui, K. Sawada, R. Yokoyama, and H. Aki, "Predictive management for energy supply networks using photovoltaics, heat pumps, and battery by two-stage stochastic programming and rule-based control," *Energy*, vol. 179, pp. 1302–1319, Jul. 2019, doi: 10.1016/j.energy.2019.04.148.

[113] H. Wolisz *et al.*, "Cost optimal sizing of smart buildings' energy system components considering changing end-consumer electricity markets," *Energy*, vol. 137, pp. 715–728, Oct. 2017, doi: 10.1016/j.energy.2017.06.025.

[114] M. Stadler *et al.*, "THE CO2 ABATEMENT POTENTIAL OF CALIFORNIA'S MID-SIZED COMMERCIAL BUILDINGS," LBNL-3024E, 972651, Dec. 2009. doi: 10.2172/972651.

[115] C. Roselli, M. Sasso, and F. Tariello, "Dynamic Simulation of a Solar Electric Driven Heat Pump Integrated with Electric Storage for an Office Building Located in Southern Italy," *Int. J. Heat Technol.*, vol. 34, no. 4, pp. 637–646, Dec. 2016, doi: 10.18280/ijht.340413.

[116] L. Yang, N. Tai, C. Fan, and Y. Meng, "Energy regulating and fluctuation stabilizing by air source heat pump and battery energy storage system in microgrid," *Renew. Energy*, vol. 95, pp. 202–212, Sep. 2016, doi: 10.1016/j.renene.2016.04.019.

[117] J. von Appen and M. Braun, "Sizing and Improved Grid Integration of Residential PV Systems With Heat Pumps and Battery Storage Systems," *IEEE Trans. Energy Convers.*, vol. 34, no. 1, pp. 562–571, Mar. 2019, doi: 10.1109/TEC.2019.2892396.

[118] T. Beck, H. Kondziella, G. Huard, and T. Bruckner, "Optimal operation, configuration and sizing of generation and storage technologies for residential heat pump systems in the spotlight of self-consumption of photovoltaic electricity," *Appl. Energy*, vol. 188, pp. 604–619, Feb. 2017, doi: 10.1016/j.apenergy.2016.12.041.

[119] "Maximum demand charge rates for commercial and industrial electricity tariffs in the United States - OpenEI DOE Open Data." https://openei.org/doe-opendata/dataset/maximum-demand-charge-rates-for-commercial-and-industrial-electricity-tariffs-in-the-united-sta181 (accessed Oct. 15, 2020).

[120] T. Deetjen, A. Reimers, and M. Webber, "Can storage reduce electricity consumption? A general equation for the grid-wide efficiency impact of using cooling thermal energy storage for load shifting," *Environ. Res. Lett.*, vol. 13, Dec. 2017, doi: 10.1088/1748-9326/aa9f06.

[121] P. Mishra *et al.*, "A Framework to Analyze the Requirements of a Multi-Port, Megawatt-Level Charging Station for Heavy-Duty Electric Vehicle," presented at the 99th Transportation Research Board Annual Meeting, Washington D.C., Jan. 2020.

[122] E. Y. Ucer, M. C. Kisacikoglu, F. Erden, A. Meintz, and C. Rames, "Development of a DC Fast Charging Station Model for use with EV Infrastructure Projection Tool," in *2018 IEEE Transportation Electrification Conference and Expo (ITEC)*, Jun. 2018, pp. 904–909, doi: 10.1109/ITEC.2018.8450158.

[123] E. Wood, S. Raghavan, C. Rames, J. Eichman, and M. Melaina, *Regional Charging Infrastructure for Plug-In Electric Vehicles: A Case Study of Massachusetts*. 2017.

[124] N. DeForest, G. Mendes, M. Stadler, W. Feng, J. Lai, and C. Marnay, "Optimal deployment of thermal energy storage under diverse economic and climate conditions," *Appl. Energy*, vol. 119, pp. 488–496, Apr. 2014, doi: 10.1016/j.apenergy.2014.01.047.

[125] R. Fu, T. W. Remo, and R. M. Margolis, "2018 U.S. Utility-Scale Photovoltaics-Plus-Energy Storage System Costs Benchmark," National Renewable Energy Lab. (NREL), Golden, CO (United States), NREL/TP-6A20-71714, Nov. 2018. doi: 10.2172/1483474.